

# Efficient Shortest Path Queries on 3D Weighted Terrain Surfaces for Moving Objects

Yinzhaoyan Yan

The Hong Kong University of Science and Technology  
yyanas@cse.ust.hk

Raymond Chi-Wing Wong

The Hong Kong University of Science and Technology  
raywong@cse.ust.hk

**Abstract**—Studying the shortest path query for moving objects on a terrain surface has aroused widespread concern in industry and academia. In this paper, we study the *weighted region problem*, which aims at finding the shortest path between two points passing different regions on a 3D weighted terrain surface and different regions are assigned different weights. We propose an efficient  $(1 + \epsilon)$ -approximate on-the-fly algorithm to solve it. Our experimental results show that our algorithm is up to 1630 times and 40 times better than the best-known algorithm in terms of running time and memory usage in realistic settings<sup>1</sup>.

## I. INTRODUCTION

The shortest path query for moving objects becomes increasingly widespread nowadays [6], [28], especially on terrain datasets. In industry, many companies and applications, including Metaverse and Google Earth, use terrain datasets (e.g., mountains and valleys) with different features (e.g., water and forest) to help moving users compute the shortest path to the destination. In academia, the shortest path query on terrain datasets is a prevalent research topic in the field of mobile data management [11], [13], [14], [29], [30], [31], [32], [33]. A terrain surface contains a set of *faces* each of which is denoted by a triangle. Each face consists of three *edges* connecting at three *vertices*. The *weighted* (resp. *unweighted*) *shortest path* on a terrain surface means the shortest path between a source  $s$  and a destination  $t$  passing on the face of the terrain where each face is assigned with a *weight* (resp. each face weight is set to a fixed value, e.g., 1). Figures 1 (a) and (b) show a real map and a terrain surface (of Valais, Switzerland [3] with an area of 20km<sup>2</sup>) with weighted (resp. unweighted) shortest paths in the blue (resp. purple dashed) line from  $s$  to  $t$ .

### A. Motivation

Computing the weighted shortest path on terrain surfaces between two points is involved in numerous applications with different interpretations of the faces' weights on the terrain.

1) **Earthquake and avalanche:** After an earthquake or avalanche, rescue teams (as moving objects) need to efficiently find the shortest rescue paths for life-saving, and they can save 1 life every 5 minutes [20]. The death toll of the 7.6 magnitude earthquake on Jan 1, 2024 in Japan exceeded 200 [2]. The 4.1 magnitude earthquake on Oct 24, 2016 in Valais, Switzerland [3] caused an avalanche. In Figures 1 (a) and (b), the terrain surface consists of destroyed regions (the

faces with green color) and non-destroyed regions (the faces with white color). Since the rescue time for passing through the destroyed region is longer than the non-destroyed region, we set the weight of each terrain face equal to the *damage level* [27] of each region, i.e., destroyed (resp. non-destroyed) regions' terrain faces will have a larger (resp. smaller) weight. The purple dashed (resp. blue) path between  $s$  (a rescue center) and  $t$  (a destroyed village) has a *weighted distance* of 109km (resp. 5.1km), so the rescue team will choose the blue path (with a smaller weighted distance) that does not pass the destroyed region. Our case study shows that the rescue time of using the purple dashed (resp. blue) path is 1.4 hours (resp. 3 min). We cannot pre-compute the path before the earthquake. But, after an earthquake, satellites can collect the terrain surface in 10s and USD \$48.72 [25] for a 1km<sup>2</sup> region, our algorithm can calculate a weighted shortest rescue path in 7.3s, and the rescue team can arrive at the destroyed village in  $3 \text{ min} \approx 3 \text{ min} + 10 \text{ s} + 7.3 \text{ s}$  for life-saving, which is efficient.

2) **Path Advisor:** *Path Advisor* [33] is a mobile app for calculating the shortest path between two rooms in a university campus. Figure 1 (c) shows a weighted terrain surface (which represents the floor of the building) in *Path Advisor*. For safety, the path should maintain a minimum distance (e.g., 0.2m) from obstacles. So, with a weight-distance function [33], faces on the floor closer to the aisle boundaries (resp. centers) are assigned higher (resp. lower) weights. The weighted shortest path in blue line is more realistic than the unweighted shortest path in purple dashed line, since the former path maintains a safe distance from obstacles. There are over 5,000 rooms in the university, so pre-computing the pairwise shortest paths is undesirable, even if we use an approximate oracle for indexing [30], [31]. Thus, it is necessary that the mobile app can efficiently calculate the path for real-time responses.

Motivated by these, we aim to efficiently solve the *weighted region problem*, i.e., finding the shortest path for moving objects between two points passing different regions on a 3D weighted terrain surface and different regions are assigned different weights depending on the application nature.

### B. Snell's law

Consider a weighted terrain surface  $T$  with  $n$  vertices. Let  $V$ ,  $E$  and  $F$  be the set of vertices, edges and faces of  $T$ . In Physics, when a light ray passes the boundary of two different media (e.g., air and glass), it bends at the boundary since light

<sup>1</sup>Code: <https://github.com/yanyinzhaoyan/WeightedTerrainCode>

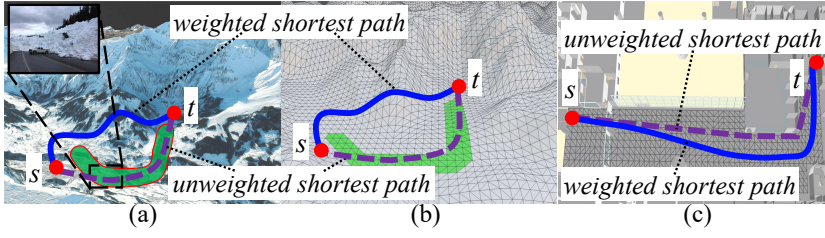


Fig. 1. Blue weighted and purple dashed unweighted shortest paths

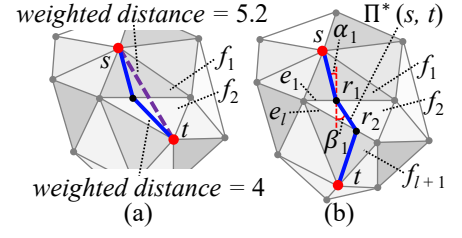


Fig. 2. Snell's law illustration

seeks the path with the minimum time. The angles of incidence and refraction for the light satisfy *Snell's law* [23], which is an important geometric information of  $T$  and can be applied to calculating the weighted shortest path (see Figures 2 (a) and (b)). In Figure 2 (a), if all faces have the same weights ( $=1$ ), the purple dashed line is the (unweighted) shortest path. When faces  $f_1$  and  $f_2$  have weights 3 and 2, the blue line with a weighted distance of 4 that satisfies Snell's law is the weighted shortest path, but the weighted distance of the purple dashed line is  $5.2 > 4$ . Figure 2 (b) shows a similar example.

### C. Challenges

No algorithm can solve the weighted region problem *exactly* when the number of faces in  $T$  exceeds two [10], but two categories of algorithms can solve it on-the-fly *approximately*.

1) **Steiner point approach:** Algorithms [4], [13], [14], [18] place discrete (i.e., Steiner) points on edges in  $E$ , and use Dijkstra's algorithm [12] on a weighted graph constructed using these Steiner points and  $V$  to calculate the result path. The best-known algorithm [13], [18] calculates a  $(1 + \epsilon)$ -approximate weighted shortest path in  $O(n^3 \log n)$  time (where  $\epsilon > 0$  is the *error parameter*), which is still very slow, since it does not utilize any geometric information on  $T$ . Algorithm [13] uses algorithm [18] as an on-the-fly algorithm to build an oracle, we regard them as one algorithm for the sake of illustration. Our experimental results show that the best-known algorithm [13], [18] runs in  $119,000s \approx 1.5$  days on a terrain surface with 50k faces.

2) **Edge sequence approach:** Algorithm [29] uses algorithm [13], [18] with slight variations (without error guarantee) to calculate a path, then uses Snell's law on the edge sequence passed by this path based on  $T$  to calculate an even shorter path. But, it does not have an error guarantee of the returned path's distance with a given time limit.

### D. Our Efficient Algorithm

We propose an efficient on-the-fly two-step algorithm for solving the 3D weighted region problem using algorithm *Rough-Refine* (*Roug-Ref*), such that for a given source  $s$  and destination  $t$  on  $T$ , it returns a  $(1 + \epsilon)$ -approximate weighted shortest path between  $s$  and  $t$ . Algorithm *Roug-Ref* is a step-by-step algorithm involving algorithm *Roug* and algorithm *Ref*. (1) In algorithm *Roug*, given  $T$ ,  $s$ ,  $t$  and  $\epsilon$ , we efficiently find a  $(1 + \eta\epsilon)$ -approximate *rough path* between  $s$  and  $t$  using Steiner points, where  $\eta > 1$  is a constant and is calculated based on  $T$  and  $\epsilon$  (note that  $\eta \in (1, 2]$  on average in our

experiments), as shown in Figures 3 (a) to (d). (2) In algorithm *Ref*, given the rough path, we efficiently *refine* it to be a  $(1 + \epsilon)$ -approximate weighted shortest path using Snell's law, as shown in Figures 3 (e) to (i). Algorithm *Roug-Ref* achieves outstanding performance in terms of running time and memory usage due to the rough-refine concept, i.e., (1) a *novel* pruning step in algorithm *Roug* during the rough path calculation with error guarantee (achieved by transferring the pruned-out information from algorithm *Roug* to algorithm *Ref*, and after conducting necessary checks in algorithm *Ref*, there is no need to perform calculations on the pruned-out information anymore), (2) an *efficient* reduction of the search area in algorithm *Roug* before Snell's law refinement (achieved by the calculation of the rough path), and (3) the usage of *Snell's law* in algorithm *Ref* for efficient refinement.

We have four additional novel techniques for further speedup, including (1) an *efficient* Steiner point placement scheme in algorithm *Roug* for reducing the number of Steiner points during the rough path calculation (achieved by considering geometric information of each face in  $F$  on  $T$ , such as face weight, internal angle and edge length), (2) a *progressive* approach in algorithm *Ref* for minimizing the search area before Snell's law refinement (achieved by progressively exploring the local search area instead of directly using the global search area), (3) an *effective weight* pruning technique in algorithm *Ref* for faster processing during Snell's law refinement (achieved by considering additional information on  $T$ ), and (4) a *novel* error guaranteed pruning technique in algorithm *Ref* for handling rare cases when we are unable to use Snell's law to refine a rough path to a  $(1 + \epsilon)$ -approximate weighted shortest path, then an additional step is required for error guarantee, but the algorithm total running time will not increase a lot (achieved by re-using the calculated information in algorithm *Roug*).

In Section I-A, we prioritize algorithm efficiency and we can tolerate an error. For the earthquake rescue, our calculated weighted shortest rescue path has  $\epsilon = 0.05$ , i.e., the rescue time of using the exact weighted shortest rescue path is at least  $2.86 (= \frac{3}{1.05})$  min, but it takes  $7,900s \approx 2.2$  hours to calculate a path with  $\epsilon = 0.01$  using the same algorithm.

### E. Contributions and Organization

We summarize our major contributions.

(1) We are the first to propose the efficient algorithm *Roug-Ref*, since the rough-refine concept and four additional techniques are absent in algorithms [4], [13], [14], [18], [29].

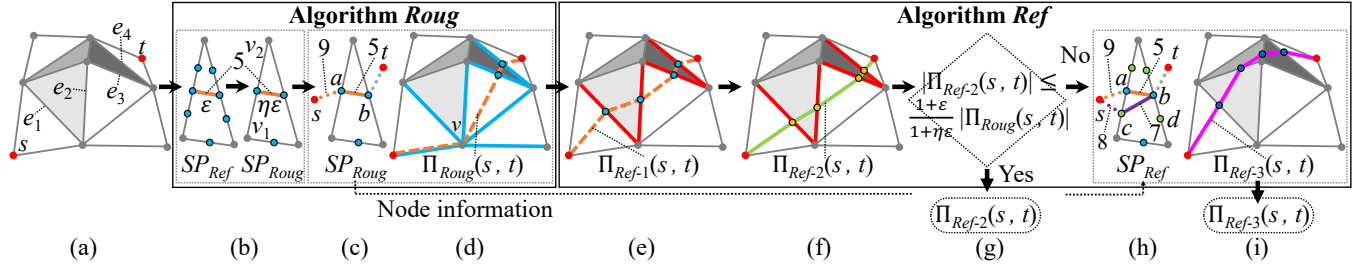


Fig. 3. Framework overview

(2) We provide a thorough theoretical analysis on the running time, memory usage and error bound of our algorithm.

(3) Our experimental results show that our algorithm runs up to 1630 times faster than the best-known algorithm [13], [18] on benchmark real datasets with the same error ratio, e.g., for a terrain surface with 50k faces with  $\epsilon = 0.1$ , our algorithm runs in 73s  $\approx$  1.2 min and uses 43MB of memory, but the best-known  $(1 + \epsilon)$ -approximate algorithm [13], [18] runs in 119,000s  $\approx$  1.5 days and uses 2.9GB of memory. Our algorithm is the optimal algorithm in earthquake rescue.

The remainder of the paper is organized as follows. Section II provides the preliminary. Section III covers the related work. Section IV presents our algorithm. Section V presents the experimental results and Section VI concludes the paper.

## II. PRELIMINARY

### A. Notations and Definitions

1) **Terrain surfaces and paths:** Consider a weighted terrain surface  $T$  with  $n$  vertices. Let  $V$ ,  $E$  and  $F$  be the set of vertices, edges and faces of  $T$ . Each vertex  $v \in V$  has three coordinate values,  $x_v$ ,  $y_v$  and  $z_v$ . Let  $L$  be the length of the longest edge of  $T$ , and  $N$  be the smallest integer value that is larger than or equal to the coordinate value of any vertex in  $V$ . If two faces share a common edge, they are said to be *adjacent*. Each face  $f_i \in F$  is assigned a weight  $w_i > 0$ , and the weight of an edge is the smaller weight of the two faces containing the edge. The maximum and minimum weights of the face in  $F$  are denoted by  $W$  and  $w$ . The minimum height of a face in  $F$  is denoted by  $h$ . Given a face  $f_i$ , and two points  $p$  and  $q$  on  $f_i$ , let  $\overline{pq}$  be a line segment between  $p$  and  $q$  on  $f_i$ ,  $d(p, q)$  be the Euclidean distance between  $p$  and  $q$  on  $f_i$ , and  $D(p, q) = w_i \cdot d(p, q)$  be the *weighted (surface) distance* from  $p$  to  $q$  on  $f_i$ . Given  $s$  and  $t$  in  $V$ , let  $\Pi^*(s, t) = (s, r_1, \dots, r_l, t)$  be the *optimal weighted shortest path* on  $T$  (with  $l \geq 0$ ) such that  $\sum_{i=0}^l D(r_i, r_{i+1})$  is the minimum, where  $r_0 = s$  and  $r_{l+1} = t$ . Here, for each  $i \in \{1, \dots, l\}$ ,  $r_i$  is a point on an edge in  $E$ , is named as an *optimal intersection point* in  $\Pi^*(s, t)$ . The blue path in Figure 2 (b) shows an example of  $\Pi^*(s, t) = (s, r_1, r_2, t)$  on  $T$ . We define  $|\cdot|$  to be the weighted distance of a path, e.g.,  $|\Pi^*(s, t)|$  is the weighted distance of  $\Pi^*(s, t)$ . Let  $\Pi(s, t)$  be the path result of our algorithm. If point  $s$  (or  $t$ ) is not in  $V$ , we can regard it as a new vertex and then add three new triangles each involving this point and three vertices of the face containing this point. A notation table can be found in the appendix of Table III.

2) **Snell's Law:** Let  $S = ((v_1, v'_1), \dots, (v_l, v'_l)) = (e_1, \dots, e_l)$  be a sequence of edges that  $\Pi^*(s, t)$  connects from  $s$  to  $t$  in order based on  $T$ , where  $S$  is said to be *passed by*  $\Pi^*(s, t)$ . Let  $l$  be the number of edges in  $S$ . Let  $F(S) = (f_1, f_2, \dots, f_l, f_{l+1})$  be an adjacent face sequence corresponds to  $S$ , such that for every  $f_i$  with  $i \in \{2, \dots, l\}$ ,  $f_i$  is the face that contains  $e_i$  and  $e_{i+1}$  in  $S$ , while  $f_1$  is the face that adjacent to  $f_2$  at  $e_1$  and  $f_{l+1}$  is the face that adjacent to  $f_l$  at  $e_l$ . We define  $\alpha_i$  and  $\beta_i$  to be the incidence and refraction angles of  $\Pi^*(s, t)$  on  $e_i$  for  $i \in \{1, \dots, l\}$ , respectively. In Figure 2 (b),  $\Pi^*(s, t)$  stratifies Snell's law,  $w_i \cdot \sin \alpha_i = w_{i+1} \cdot \sin \beta_i$ , with  $i \in \{1, \dots, l\}$ .

### B. Problem

Given  $T$ ,  $s$  and  $t$ , the problem is to calculate a weighted shortest path on  $T$  such that  $|\Pi(s, t)| \leq (1 + \epsilon)|\Pi^*(s, t)|$ .

## III. RELATED WORK

### A. On-the-fly algorithms on the weighted terrain surface

1) **Steiner point approach:** Algorithms [4], [13], [14], [18] use Dijkstra's algorithm on the weighted graph constructed using Steiner points and  $V$  to calculate an approximate weighted shortest path. Algorithm *Fixed Steiner Point (FixSP)* [13], [18] and algorithm *Fixed Steiner Point No Weight Adaption (FixSP-NoWei-Adp)* [14] (resp. algorithm *Logarithmic Steiner Point (LogSP)* [4]) calculates the result path with an error  $(1 + \epsilon)$  (resp. much larger than  $(1 + \epsilon)$ ). (i) Algorithm *FixSP* places a uniform number of Steiner points (i.e.,  $O(n^2)$ ) per edge. It runs in  $O(n^3 \log n)$  time and is regarded as the best-known  $(1 + \epsilon)$ -approximate algorithm for solving the weighted region problem. (ii) Algorithm [14] also places a uniform number of Steiner points per edge, but it was originally designed in the unweighted case. We adapt it to be algorithm *FixSP-NoWei-Adp* [14] in the weighted case, which runs in  $O(n^3 \log n)$  time and equivalent to *FixSP*, by assigning a weight to each face, and use the same surface distance definition in Section II-A1. (iii) In algorithm *LogSP*, given an error parameter  $\epsilon' > 0$  that determines how far the Steiner points are placed (different from our  $\epsilon$  that controls the distance error bound), it places  $O(\log \frac{c}{\epsilon'})$  Steiner points per edge non-uniformly, i.e., places more (resp. less) Steiner points near (resp. far away from) a vertex, and has a distance error  $(1 + (2 + \frac{2W}{(1-2\epsilon') \cdot w})\epsilon')$ , where  $c \in [0.2, 1]$  is a constant depending on  $T$ . We adapt it to be algorithm *LogSP-Adp* that runs in  $O(n \log \frac{c}{\epsilon} \log(n \log \frac{c}{\epsilon}))$ .

time, such that given  $\epsilon$ , we can place Steiner points using  $\epsilon$  and have a distance error  $(1 + \epsilon)$ , by finding the relationship between  $\epsilon$  and  $\epsilon'$ , so these two algorithms can place the same number of Steiner points per edge, and their distance errors are the same, i.e.,  $1 + (2 + \frac{2W}{(1-2\epsilon') \cdot w})\epsilon' = 1 + \epsilon$ , and get  $\epsilon' = \frac{1+\epsilon+\frac{W}{w}-\sqrt{(1+\epsilon+\frac{W}{w})^2-4\epsilon}}{4}$ .

**Drawbacks of algorithm *FixSP* and *FixSP-NoWei-Adp*:** They are very slow due to two reasons. (i) *Absence of Snell's law*: They do not utilize any geometric information *between two adjacent faces in  $F$  that share one edge on  $T$* , i.e., Snell's law. So, they place many Steiner points on edges in  $E$ . But, we utilize Snell's law to avoid this. (ii) *Uniform number of Steiner points per edge*: They do not utilize any geometric information of *each face in  $F$  on  $T$* , such as face weight, internal angle and edge length, and always place a uniform number of Steiner points (i.e.,  $O(n^2)$ ) per edge (the distance between two adjacent Steiner points on the same edge is the same) to bound the error. But, we utilize this information and place only  $O(\log c')$  Steiner points per edge (the distance between two adjacent Steiner points on the same edge is different), where  $c' \in [2, 5]$  is a constant depending on  $T$  and  $\epsilon$ . Figures 4 (a) and (b) show the placement of Steiner points in these two algorithms and our algorithm *Roug-Ref* with the same error. Our experimental results show that for a terrain surface with 50k faces and  $\epsilon = 0.1$ , *Roug-Ref* just places 10 Steiner points per edge to find a rough path in 71s  $\approx 1.2$  min, and finds a refined path in 2s, but both *FixSP* and *FixSP-NoWei-Adp* place more than 600 Steiner points per edge to find the result path in 119,000s  $\approx 1.5$  days.

**Drawback of algorithm *LogSP* and *LogSP-Adp*:** (i) *LogSP* has the *larger distance error* drawback, since its distance error is always larger than that of other algorithms, making it difficult to compare with other algorithms. (ii) Both of them also have the *absence of Snell's law* drawback. In the same experimental setting of the previous paragraph, *Roug-Ref* runs in 73s  $\approx 1.2$  min, but *LogSP-Adp* runs in 220s  $\approx 3.7$  min.

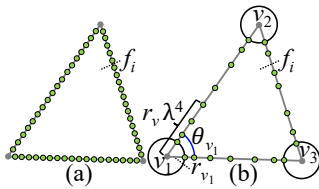


Fig. 4. Steiner points in (a) *FixSP* and *FixSP-NoWei-Adp*, and (b) *Roug-Ref*

2) **Edge sequence approach**: Algorithm *Edge Sequence* (*EdgSeq*) [29] uses *FixSP* with only slight variations (i.e., places a uniform and constant number of Steiner points, e.g., 3 and not  $O(n^2)$ , per edge) to calculate a path without error guarantee, then uses Snell's law on the edge sequence passed by this path based on  $T$  to calculate a shorter path. We adapt it to be algorithm *EdgSeq-Adp*, that uses *FixSP* to calculate a  $(1 + \epsilon)$ -approximate shortest path, then uses Snell's law on the edge sequence of this path to compute a shorter path that runs in  $O(n^3 \log n + n^4 \log(\frac{n^2 NWL}{w\epsilon}))$  time.

**Drawbacks of algorithm *EdgSeq* and *EdgSeq-Adp*:** (i) *EdgSeq* does not have an error guarantee of the returned path's distance with a given time limit. (ii) *EdgSeq-Adp* is still very slow due to two reasons. (1) *Absence of pruning technique for the edge sequence finding*: It uses Snell's law after *FixSP*, so its running time is an additive result of the running time of *FixSP* and usage of Snell's law. But, we use a pruning technique to further prune out more than half of the Steiner points. (2) *Absence of pruning technique when using Snell's law*: It solely uses binary search in Snell's law on the edge sequence. But, we use *effective weight* information of  $T$  for pruning. In the same experimental setting of the previous three paragraphs, *EdgSeq-Adp* runs in 131,000s  $\approx 1.7$  days, but *Roug-Ref* runs in 73s  $\approx 1.2$  min. If we substitute *FixSP* to *LogSP-Adp* in *EdgSeq-Adp*, the new algorithm has the same drawback as of *EdgSeq-Adp*, and its running time is always larger than that of *LogSP-Adp*, so there is no need to consider this adaption.

**Comparisons:** We compare different algorithms in Table I. *Roug-Ref* has the smallest query time and memory usage.

#### B. Other related studies

There are some other studies related to our problem but are not exactly our problem. (1) *On-the-fly algorithms on the unweighted terrain surface* [8]: Algorithm [8] is the best-known exact on-the-fly algorithm for the unweighted shortest path calculation, but no known algorithm can adapt it to the weighted case. (2) *Oracles on the terrain surface* [11], [13], [26], [30], [31], [32]: Study [13] uses algorithm *FixSP* [18] (resp. studies [30], [31] use algorithm [14]) to pre-compute the weighted (resp. unweighted) shortest paths and build an oracle on a weighted (resp. unweighted) terrain surface for the shortest path query. Studies [11], [26], [32] build oracles on an unweighted terrain surface for the k-nearest neighbor query. But, we focus on the *on-the-fly* algorithm, which is a fundamental operator for oracle construction. (3) *On-the-fly algorithms on the road network* [6], [28]: Algorithms [6], [28] answer the shortest path query on the road network, which is totally different from us.

## IV. METHODOLOGY

### A. Overview

1) **Concepts**: We give four concepts:

(i) **The weighted graph**: It is used in Dijkstra's algorithm. Let  $G_A$  be a weighted graph used in algorithm *Roug* or *Ref*,  $G_A.V$  and  $G_A.E$  be the sets of nodes and weighted edges of  $G_A$ , where  $A$  is a placeholder that can be *Roug* or *Ref*. To build  $G_A$ , we define a set of Steiner points on each edge of  $E$  as  $SP_A$ . Let  $G_A.V = SP_A \cup V$ . For each node  $p$  and  $q$  in  $G_A.V$ , if  $p$  and  $q$  lie on the same face in  $F$ , we connect them with a weighted edge  $\overline{pq} \in G_A.E$ , with the weighted (surface) distance  $w_{pq} \cdot d(p, q)$ , where  $w_{pq}$  means the weight associated with the face or the edge that  $p$  and  $q$  lie on. In Figure 3 (b), the blue nodes are  $SP_{Ref}$  and  $SP_{Roug}$ , the blue and gray nodes are  $G_{Ref}.V$  and  $G_{Roug}.V$ , the orange lines are the weighted edge with weighted distance 5 in  $G_{Roug}.E$  and  $G_{Ref}.E$ .

TABLE I  
ALGORITHM COMPARISONS

| Algorithm                     | Time/Size    | Error        |
|-------------------------------|--------------|--------------|
| <i>EdgSeq</i> [29]            | Large        | Large        |
| <i>EdgSeq-Adp</i> [29]        | Large        | Small        |
| <i>FixSP</i> [13], [18]       | Large        | Small        |
| <i>FixSP-NoWei-Adp</i> [14]   | Large        | Small        |
| <i>LogSP</i> [4]              | Medium       | Large        |
| <i>LogSP-Adp</i> [4]          | Medium       | Small        |
| <b><i>Roug-Ref</i> (ours)</b> | <b>Small</b> | <b>Small</b> |



(ii) **The removing value:** It is a constant (denoted by  $k$  and usually set to 2) used for calculating  $SP_{Roug}$ . In Figure 3 (b), we have a set of Steiner points  $SP_{Ref}$ . When moving from  $v_1$  to  $v_2$ , if we encounter a Steiner point, we iteratively keep one and remove the next  $k = 1$  point(s). We repeat it for all edges in  $E$  to obtain a set of remaining Steiner points  $SP_{Roug}$ .

(iii) **The node information:** It is calculated in algorithm *Roug*, and is used to reduce the running time in algorithm *Ref*. In Dijkstra's algorithm, given a source node  $s$ , a set of nodes  $G_A.V$  where  $A$  can be *Roug* or *Ref*, for each  $u \in G_A.V$ , we define  $dist_A(u)$  to be the weighted shortest distance from  $s$  to  $u$ , define  $prev_A(u)$  to be the previous node of  $u$  along the weighted shortest path from  $s$  to  $u$ . Give  $s$ , after running algorithm *Roug*, node information stores  $dist_{Roug}(u)$  and  $prev_{Roug}(u)$  (based on  $s$ ) for each  $u \in G_{Roug}.V$ . In Figure 3 (c), suppose that the weight of this face is 1. After running algorithm *Roug*, the weighted shortest distance from  $s$  to  $a$  is 9, the Euclidean distance of the orange edge is 5, the weighted shortest path from  $s$  to  $b$  is  $s \rightarrow a \rightarrow b$ , so we have  $dist_{Roug}(b) = 9 + 1 \times 5 = 14$  and  $prev_{Roug}(b) = a$  as node information of  $b$ .

(iv) **The full or non-full edge sequence:** Given an edge sequence  $S$ , if the length of each edge in  $S$  is larger than 0 (resp. there exists at least one edge in  $S$  whose length is 0), then  $S$  is a *full* (resp. *non-full*) edge sequence or  $S$  is *full* (resp. *non-full*). In Figure 5 (a), given the path in the purple dashed (resp. orange) line between  $s$  and  $t$ , the edge sequence passed by this path is full (resp. non-full) since the length of each edge is larger than 0 (resp. the edge length at  $\phi_2, \phi_3$  and  $\phi_4$  are 0). Figure 5 (b) has a similar case. As we will discuss later, a full (resp. non-full) edge sequence reduces (resp. increases) algorithm *Ref*'s running time.

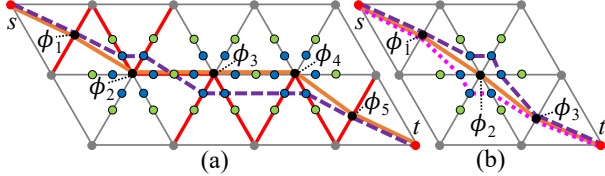


Fig. 5. Full edge sequence conversion

2) **Overview of algorithm *Roug*:** Given  $T, s, t, \epsilon$  and  $k$ , we find a  $(1 + \eta\epsilon)$ -approximate rough path between  $s$  and  $t$ , and calculate the node information for  $s$  in two steps:

(i)  **$\eta$  calculation:** In Figure 3 (a), given  $T, \epsilon$  and  $k$ , we first use  $\epsilon$  and an efficient Steiner point placement scheme to get  $SP_{Ref}$ , and then use  $k$  to remove some Steiner points and get  $SP_{Roug}$  in Figure 3 (b), and then use  $SP_{Roug}$  to calculate  $\eta\epsilon$ .

(ii) **Rough path calculation:** In Figure 3 (c), given  $T, s, t$  and  $SP_{Roug}$ , we use Dijkstra's algorithm on  $G_{Roug}$  constructed by  $SP_{Roug}$  and  $V$  (we must include  $V$  in  $SP_{Roug}$  for error guarantee) to calculate a  $(1 + \eta\epsilon)$ -approximate rough path between  $s$  and  $t$  in Figure 3 (d) (denoted by  $\Pi_{Roug}(s, t)$ , i.e., the orange dashed line), and store  $dist_{Roug}(u)$  and  $prev_{Roug}(u)$  (based on  $s$ ) for each  $u \in G_{Roug}.V$  as node information.

3) **Overview of algorithm *Ref*:** Given  $T, s, t, \epsilon, \Pi_{Roug}(s, t)$  and the node information, we refine  $\Pi_{Roug}(s, t)$  and calculate

a  $(1 + \epsilon)$ -approximate weighted shortest path in four steps:

(i) **Full edge sequence conversion:** In Figure 3 (d), given  $\Pi_{Roug}(s, t)$  whose corresponding edge sequence  $S'$  is non-full (the edge length at  $v$  is 0), we progressively convert it to a modified rough path in Figure 3 (e) (denoted by  $\Pi_{Ref-1}(s, t)$ , i.e., the orange dashed line) whose corresponding edge sequence  $S = (e_1, e_2, e_3, e_4)$  (edges in red) is full.

(ii) **Snell's law path refinement:** In Figure 3 (f), given  $T, s, t$  and  $S$ , we use Snell's law and  $S$  to efficiently get a refined path (denoted by  $\Pi_{Ref-2}(s, t)$ , i.e., the green line) on  $S$ .

(iii) **Path checking:** In Figure 3 (g), given  $\Pi_{Roug}(s, t)$ ,  $\Pi_{Ref-2}(s, t)$ ,  $\epsilon$  and  $\eta$ , if  $|\Pi_{Ref-2}(s, t)| \leq \frac{(1+\epsilon)}{(1+\eta\epsilon)} |\Pi_{Roug}(s, t)|$ , since we guarantee  $|\Pi_{Roug}(s, t)| \leq (1 + \eta\epsilon) |\Pi^*(s, t)|$  due to the error bound of Dijkstra's algorithm (see Theorem 3.1 of study [17]), we have  $|\Pi_{Ref-2}(s, t)| \leq (1 + \epsilon) |\Pi^*(s, t)|$ , and we return  $\Pi_{Ref-2}(s, t)$ . Otherwise, we need the next step.

(iv) **Error guaranteed path refinement:** In Figures 3 (h), given  $T, s, t, SP_{Ref}$  and the node information (based on  $s$ ), we use Dijkstra's algorithm on  $G_{Ref}$  constructed by  $SP_{Ref}$  and  $V$  to efficiently calculate a  $(1 + \epsilon)$ -approximate weighted shortest path between  $s$  and  $t$  in Figure 3 (i) (denoted by  $\Pi_{Ref-3}(s, t)$ , i.e., the purple line). We can guarantee  $|\Pi_{Ref-3}(s, t)| \leq (1 + \epsilon) |\Pi^*(s, t)|$  due to the error bound of Dijkstra's algorithm.

## B. Key Ideas of Rough-Refine Concept

Algorithm *Roug-Ref* is efficient due to the rough-refine concept, which involves the following three techniques.

1) **Novel Steiner point pruning step (in the  $\eta$  calculation step):** In Figure 3 (b), we prune out some Steiner points in  $SP_{Ref}$  using  $k$ , and use the remaining Steiner points  $SP_{Roug}$  for the rough path calculation, i.e.,  $SP_{Roug} \subseteq SP_{Ref}$  and  $G_{Roug}.V \subseteq G_{Ref}.V$ . The pruned Steiner points are transferred to the error guaranteed path refinement step, and our experimental results show that it is very likely after the Snell's law path refinement, the path checking finds that there is no need to perform Dijkstra's algorithm on these pruned Steiner points.

2) **Efficient reduction of the search area (in the rough path calculation step):** In Figure 3 (d), the edge sequence  $S'$  passed by  $\Pi_{Roug}(s, t)$  is used in the Snell's law path refinement step. If we do not know  $S'$ , we need to try Snell's law on different combinations of edges in  $E$  (so the search area is large) and select the shortest result path, which is time-consuming.

3) **Usage of Snell's law (in the Snell's law path refinement step):** In Figure 3 (e), we utilize Snell's law on  $S'$  to efficiently calculate  $\Pi_{Ref-2}(s, t)$ , such that the distance between the intersection point of  $\Pi_{Ref-2}(s, t)$  on each edge of  $S'$  and that of  $\Pi^*(s, t)$  is smaller than an error value  $\delta = \frac{h_{ew}}{6lW}$ , and there is no need to place many Steiner points on edges in  $E$ .

## C. Key Ideas of Additional Techniques

We also have the following four additional novel techniques to make algorithm *Roug-Ref* more efficient.

1) **Efficient Steiner point placement scheme with a  $(1 + \epsilon)$  error bound (in the  $\eta$  calculation step):** In Figures 3 (b) and 4 (b), we have an efficient Steiner point placement scheme (i) by considering the additional geometric information of  $T$ , such

as face weight, internal angle, and edge length, etc., so that we can place *different* numbers of Steiner points on different edges of  $E$  (for minimizing the total number of Steiner points), and (ii) by using mathematical transformations to express the error in terms of  $(1 + \epsilon)$  (so that with the  $\eta$  calculation step, the rough path has an error  $(1 + \eta\epsilon)$ ).

2) **Novel full edge sequence conversion technique using progressive approach** (in the full edge sequence conversion step): In Figure 3 (d),  $S'$  passed by  $\Pi_{Roug}(s, t)$  is non-full at vertex  $v$ . If we use Snell's law on  $S'$  to calculate a refined path, after the path exits  $v$ , we do not know where it goes next, so we need to add *all* the edges connected to  $v$  in  $S'$  (edges in blue) for error guarantees, and try Snell's law on different combinations of edge sequences to select the shortest result path. Indeed, only a subset of these edges is required. To solve it, we need the full edge sequence conversion step.

**Illustration:** In Figure 5 (a), given a rough path  $(s, \phi_1, \phi_2, \phi_3, \phi_4, \phi_5, t)$  (i.e., the orange line) whose corresponding edge sequence is non-full, we divide it into a smaller segment  $(\phi_1, \phi_2, \phi_3, \phi_4, \phi_5)$  that all the edges passed by this segment have length equal to 0, i.e., at  $\phi_2, \phi_3$  and  $\phi_4$ . We add more Steiner points to *progressively* find a new path segment, i.e., the purple dashed line between  $\phi_1$  and  $\phi_5$ , until the edge sequence (in red) passes by this path segment is full. If the distance of the new path segment is smaller than that of the original one, we replace the new one with the original one, and obtain a modified rough path (i.e., the purple dashed line between  $s$  and  $t$ ). Figure 5 (b) shows a similar example.

3) **Novel effective weight pruning technique** (in the Snell's law path refinement step): In Figure 3 (f), we use Snell's law to find optimal intersection points on each edge of  $S$ , then connect them to form  $\Pi_{Ref-2}(s, t)$ . The basic idea is to use binary search, but we can efficiently prune out some checking by utilizing *effective weight* information on  $T$ .

**Illustration:** In Figure 6 (a), we select the midpoint  $m_1$  on  $e_1$ , and trace a blue light ray that follows Snell's law from  $s$  to  $m_1$ . We use binary search to adjust the position of  $m_1$  to the left or right by checking whether  $t$  is on the left or right of this ray, and repeat until the ray passes the entire  $S$ , i.e., the purple ray from  $s$  to  $m_1^1$ . In Figure 6 (b), we regard all the faces in  $F(S)$  except  $f_1$  as one *effective face*  $\Delta_{u_p p_1 q_1}$ , and use the ray in the purple line for calculating its effective weight. Then, we can calculate the position of  $m_{ef}$  on  $e_1$  in one quartic equation using the weight of  $f_1$  and the effective weight of  $\Delta_{u_p p_1 q_1}$ . In Figure 6 (c), we trace the ray starting from  $s$  and passing  $m_{ef}$  (i.e., the dark blue line). We iterate the midpoint selection step until (i) the ray hits  $t$  or (ii) the distance between the new  $m_1$  and the previous  $m_1$  is smaller than  $\delta$ . In Figure 6 (d), we continue on other edges in  $S$ .

4) **Novel error guaranteed path refinement using pruning technique** (in the error guaranteed path refinement step): In Figure 3 (g), for the path checking step, when  $k \leq 2$ , only in a rare case (i.e., the edge sequence passed by the rough path differs from that of the optimal weighted shortest path) which never occurs in our experiments, we need the error guaranteed path refinement step in Figures 3 (h) and (i). When

$k$  is larger, more Steiner points are removed, and  $\eta$  is larger, so the chance that  $|\Pi_{Ref-2}(s, t)| > \frac{(1+\epsilon)}{(1+\eta\epsilon)} |\Pi_{Roug}(s, t)|$  becomes larger, we need this step to ensure error guarantee and hope that the running time of algorithm *Roug-Ref* will not increase a lot, by using the node information.

**Illustration:** (i) In the rough path calculation step, see Figure 3 (c), we have  $dist_{Roug}(b) = 9 + 1 \times 5 = 14$  and  $prev_{Roug}(b) = a$  as node information of  $b$ . (ii) In the error guaranteed path refinement step, see Figure 3 (h), since  $G_{Roug}.V \subseteq G_{Ref}.V$ , we know  $dist_{Ref}(b) = 14$  and  $prev_{Ref}(b) = a$ . We maintain a *priority queue* [9]  $Q = \{\{u_1, dist_{Ref}(u_1)\}, \dots\}$  in Dijkstra's algorithm on  $G_{Ref}$  that stores a set of nodes  $u_i \in G_{Ref}.V$  waiting for processing. Suppose we need to process  $a$  and  $c$ , so  $Q$  stores  $\{\{a, 9\}, \{c, 8\}\}$ . We dequeue  $c$  with a shorter distance value ( $8 < 9$ ), and one adjacent node of  $c$  is  $b$ . Since  $dist_{Ref}(b) = 14 < dist_{Ref}(c) + w_{bc} \cdot d(b, c) = 8 + 1 \times 7 = 15$ , we do not need to insert  $b$  and  $dist_{Ref}(b) = 15$  into the queue for time-saving. Since  $G_{Ref}.V$  contains  $G_{Roug}.V$  and the removed Steiner points, the running time by performing Dijkstra's algorithm on  $G_{Ref}$  without the node information is the same as the time of the rough path calculation step plus the time of error guaranteed path refinement step.

#### D. Implementation Details of Algorithm Roug

We give implementation details of algorithm *Roug* (see Figures 3 (a) to (d)). We mainly discuss our efficient Steiner points placement scheme with a  $(1 + \epsilon)$  error bound, (i.e., the technique in algorithm *LogSP-Adp*).

**Detail:** Given a vertex  $v$  in  $V$ , we let  $h_v$  be the minimum height starting from  $v$  on the faces containing  $v$ , let  $C_v$  be a *sphere* centered at  $v$  with radius  $r_v = \frac{1+\epsilon+\frac{W}{w}-\sqrt{(1+\epsilon+\frac{W}{w})^2-4\epsilon}}{4} \cdot h_v$ , and let  $\theta_v$  be the angle between any two edges of  $T$  that are incident to  $v$ . In Figure 4 (b), there is a sphere  $C_{v_1}$  centered at  $v_1$ , with the radius  $r_{v_1}$  and the angle  $\theta_{v_1}$  of  $v_1$ . For each vertex  $v$  of face  $f_i$ , we place Steiner points  $p_1, p_2, \dots, p_{\tau_p-1}$  on two edges of  $f_i$  incident to  $v$ , such that  $|vp_j| = r_v \lambda^{j-1}$ , where  $\tau_p = \log_{\lambda} \frac{|e_p|}{2 \cdot r_v}$  for every integer  $2 \leq j \leq \tau_p - 1$ , and  $\lambda = (1 + \frac{1+\epsilon+\frac{W}{w}-\sqrt{(1+\epsilon+\frac{W}{w})^2-4\epsilon}}{4} \cdot \sin \theta_v)$ . Algorithm *LogSP* has  $r_v = \epsilon' \cdot h_v$  and  $\lambda = (1 + \epsilon' \cdot \sin \theta_v)$ . Since we adapt *LogSP-Adp* to be *LogSP-Adp* by setting  $\epsilon' = \frac{1+\epsilon+\frac{W}{w}-\sqrt{(1+\epsilon+\frac{W}{w})^2-4\epsilon}}{4}$ , we obtain  $r_v$  and  $\lambda$  w.r.t.  $\epsilon$ . Since  $r_v$  (as the denominator) cannot be 0, we cannot set  $\epsilon$  to 0.

#### E. Implementation Details of Algorithm Ref

We give implementation details of algorithm *Ref*.

1) **Full edge sequence conversion:** See Figures 3 (e) and 5.

**Detail and example:** A point is said to be *on the edge* (resp. *vertex*) if it lies in the internal of an edge in  $E$  (resp. it lies on the vertex in  $V$ ). In both Figures 5 (a) and (b),  $\phi_1$  is on the edge, and  $\phi_2$  is on the vertex. Algorithm 1 shows this step, and the following is an example.

(i) *Successive point:* Lines 4-14, see Figure 5 (a) with the orange path as input.  $v_s = \phi_1$  is the *start vertex* and  $v_n = \phi_5$  is the *end vertex*. The blue points are the new Steiner points.

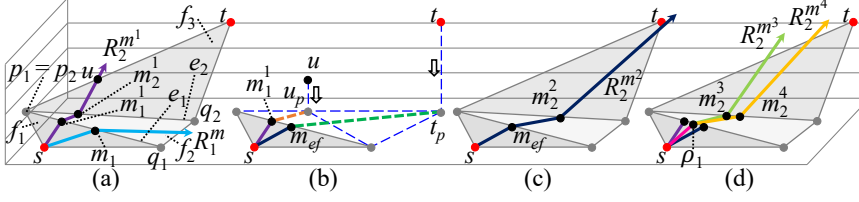


Fig. 6. Snell's law path refinement step in *Ref* (a) with initial ray for calculating effective weight on the effective face  $\Delta u_p p_1 q_1$ , (b) for calculating  $m_{ef}$ , (c) with final ray passing through  $m_{ef}$ , and (d) processing on the remaining edges

TABLE II  
DATASETS

| Name  | $ F $                   |
|---|-------------------------|
| <b>Original dataset</b>                     |                         |
| <i>BearHead</i> (BH) [30], [31]             | 280k                    |
| <i>EaglePeak</i> (EP) [30], [31]            | 300k                    |
| <i>SeaBed</i> (SB) [5]                      | 2k                      |
| <i>ValaisSwitzerland</i> (VS) [3]           | 2k                      |
| <i>PathAdvisor</i> (PA) [33]                | 1k                      |
| <b>Small-version dataset</b>                |                         |
| <i>BH</i> small-version ( <i>BH-small</i> ) | 3k                      |
| <i>EP</i> small-version ( <i>EP-small</i> ) | 3k                      |
| <b>Multi-resolution dataset</b>             |                         |
| Multi-resolution of <i>BH</i>               | 1M, 2M, 3M, 4M, 5M      |
| Multi-resolution of <i>BH-small</i>         | 10k, 20k, 30k, 40k, 50k |
| Multi-resolution of <i>EP</i>               | 1M, 2M, 3M, 4M, 5M      |
| Multi-resolution of <i>EP-small</i>         | 10k, 20k, 30k, 40k, 50k |

#### Algorithm 1 *EdgSeqConv* ( $\Pi_{Roug}(s, t)$ , $\zeta$ )

**Input:** the rough path  $\Pi_{Roug}(s, t)$  and  $\zeta$  (a constant and normally set as 10)  
**Output:** the edge sequence  $S$  of the modified rough path  $\Pi_{Ref-1}(s, t)$

- 1:  $v_s \leftarrow NULL, v_e \leftarrow NULL, E' \leftarrow \emptyset, \Pi_{Ref-1}(s, t) \leftarrow \Pi_{Roug}(s, t)$
- 2: **for** each point  $v$  that  $\Pi_{Roug}(s, t)$  intersects with an edge in  $E$  (except  $s$  and  $t$ ), such that  $v$  is on the vertex **do**
- 3:  $v_c \leftarrow v, v_n \leftarrow v_c.next, v_p \leftarrow v_c.prev$
- 4: **if**  $v_n$  is on the vertex and  $v_p$  is on the edge **then**
- 5:  $v_s \leftarrow v_c, E' \leftarrow E' \cup \text{edges with } v_c \text{ as one endpoint}$
- 6: **else if** both  $v_n$  and  $v_p$  are on the edge **then**
- 7:  $E' \leftarrow E' \cup \text{edges with } v_c \text{ as one endpoint}$
- 8: **else if**  $v_n$  is on the edge and  $v_p$  is on the vertex **then**
- 9:  $v_e \leftarrow v_n, E' \leftarrow E' \cup \text{edges with } v_c \text{ as one endpoint}$
- 10: add new Steiner points at the midpoints between the vertices and original Steiner points on  $E'$
- 11:  $\Pi'_{Roug}(v_s, v_e) \leftarrow$  path calculated using Dijkstra's algorithm on the weighted graph constructed by these new Steiner points and  $V$
- 12:  $\Pi'_{Ref-1}(v_s, v_e) \leftarrow \text{EdgSeqConv}(\Pi'_{Roug}(v_s, v_e), \zeta)$
- 13: **if**  $|\Pi'_{Ref-1}(v_s, v_e)| < |\Pi_{Roug}(v_s, v_e)|$  **then**
- 14:  $\Pi_{Ref-1}(s, t) \leftarrow \Pi_{Ref-1}(s, v_s) \cup \Pi'_{Ref-1}(v_s, v_e) \cup \Pi_{Ref-1}(v_e, t)$
- 15: **else if** both  $v_p$  and  $v_n$  are on the edge **then**
- 16: **for**  $i \leftarrow 1$  to  $\zeta$  **do**
- 17: add new Steiner points at the midpoints between  $v_c$  and the nearest Steiner points of  $v_c$  on the edges that adjacent to  $v_c$
- 18:  $\Pi_B(v_p, v_n) \leftarrow$  path passes the set of newly added Steiner points on the  $X$  side of the path  $(v_p, v_c, v_n)$ , where  $B = \{left, right\}$
- 19: **if**  $|\Pi_B(v_p, v_n)| < |\Pi_{Roug}(v_p, v_n)|$  **then**
- 20:  $\Pi_{Ref-1}(s, t) \leftarrow \Pi_{Ref-1}(s, v_p) \cup \Pi_B(v_p, v_n) \cup \Pi_{Ref-1}(v_n, t)$
- 21: **break**
- 22: **return** the edge sequence  $S$  of  $\Pi_{Ref-1}(s, t)$  based on  $T$

The orange (resp. purple dashed) line between  $\phi_1$  and  $\phi_5$  is  $\Pi_{Roug}(v_s, v_e)$  (resp.  $\Pi'_{Ref-1}(v_s, v_e)$ ).

(ii) *Single point*: Lines 15-21, see Figure 5 (b) with the orange path as input. The blue points are new Steiner points. The orange, purple line-dashed and pink dot-dashed lines between  $\phi_1$  and  $\phi_3$  are  $\Pi_{Roug}(v_p, v_n)$ ,  $\Pi_{left}(v_p, v_n)$  and  $\Pi_{right}(v_p, v_n)$ .

2) *Snell's law path refinement*: See Figures 3 (f) and 6.

**Detail and example**: Let  $\Pi_{Ref-2}(s, t) = (s, \rho_1, \dots, \rho_l, t)$ , where  $\rho_i$  for  $i \in \{1, \dots, l\}$  is a point on an edge in  $E$ . Given  $S$ ,  $s$  and a point  $c_1$  on  $e_1 \in S$ , we can obtain a *surface ray*  $\Pi_c = (s, c_1, \dots, c_g, R_g^c)$  starting from  $s$ , hitting  $c_1$  and following Snell's law on  $S$ , where  $1 \leq g \leq l$ , each  $c_i$  for  $i \in \{1, \dots, g\}$  is an intersection point in  $\Pi_c$ , and  $R_g^c$  is the last out-ray at  $e_g \in S$ . In Figure 6 (a),  $\Pi_m = (s, m_1, R_1^m)$  in blue line does not pass the whole  $S = (e_1, e_2)$ , but  $\Pi_{m^1} = (s, m_1^1, m_2^1, R_2^m)$  in purple line passes the whole  $S$ .

Algorithm 2 shows this step, and the following is an example.

#### Algorithm 2 *SneLawRef* ( $s, t, \delta, S$ )

**Input:** source  $s$ , destination  $t$ , user parameter  $\delta$  and edge sequence  $S$   
**Output:** the refined path  $\Pi_{Ref-2}(s, t)$

- 1:  $\Pi_{Ref-2}(s, t) \leftarrow \{s\}, root \leftarrow s$
- 2: **for** each  $e_i \in S$  with  $i \leftarrow 1$  to  $|S|$  **do**
- 3:  $a_i \leftarrow e_i$  left endpoint,  $b_i \leftarrow e_i$  right endpoint,  $[a_i, b_i] \leftarrow$  an interval
- 4: **for** each  $e_i \in S$  with  $i \leftarrow 1$  to  $|S|$  **do**
- 5: **while**  $|a_i b_i| \geq \delta$  **do**
- 6:  $m_i \leftarrow$  midpoint of  $[a_i, b_i]$  and calculate a surface ray with  $\Pi_m = (root, m_i, \dots, m_g, R_g^m)$  with  $g \leq l$
- 7: **if**  $\Pi_m$  does not pass the whole  $S$ , i.e.,  $g < l$  **then**
- 8: **if**  $e_{g+1}$  is on the left (resp. right) side of  $R_g^m$  **then**
- 9:  $[a_j, b_j] \leftarrow [a_j, m_j]$  (resp.  $[m_j, b_j]$ ) for each  $j \leftarrow i$  to  $g$
- 10: **else if**  $\Pi_m$  passes the whole  $S$ , i.e.,  $g = l$  **then**
- 11: **if**  $t$  is on  $R_g^m$  **then**
- 12:  $\Pi_{Ref-2}(s, t) \leftarrow \Pi_{Ref-2}(s, t) \cup \{m_i, \dots, m_g, t\}$
- 13: **return**  $\Pi_{Ref-2}(s, t)$
- 14: **else if**  $t$  is on the left (resp. right) side of  $R_g^m$  **then**
- 15:  $[a_j, b_j] \leftarrow [a_j, m_j]$  (resp.  $[m_j, b_j]$ ) for each  $j \leftarrow i$  to  $g$
- 16: **if** have not used effective weight pruning on  $e_i$  **then**
- 17:  $u \leftarrow$  the intersection point between  $R_l^m$  and one of the two edges that are adjacent to  $t$  in the last face  $f_{l+1}$  in  $F(S)$
- 18:  $u_p \leftarrow$  projected point of  $u$  on the first face  $f_1$  in  $F(S)$
- 19:  $f_{ef} \leftarrow$  effective face contains all faces in  $F(S) \setminus \{f_1\}$
- 20:  $w_{ef} \leftarrow$  effective weight for  $f_{ef}$ , calculated using  $sm_i, \bar{m}_i u_p, f_1, f_{ef}, w_1$  (the weight for  $f_1$ ) and Snell's law
- 21:  $t_p \leftarrow$  the projected point of  $t$  on  $f_1$
- 22:  $m_{ef} \leftarrow$  effective intersection point on  $e_1$ , calculated using  $w_1, w_{ef}, s, t_p$  and Snell's law in a quartic equation
- 23:  $m_i \leftarrow m_{ef}$ , compute  $\Pi_m = (root, m_i, \dots, m_g, R_g^m)$
- 24: update  $[a_j, b_j]$  for each  $j \leftarrow i$  to  $g$  same as in lines 11-15
- 25:  $\rho_i \leftarrow [a_i, b_i]$  midpoint,  $\Pi_{Ref-2}(s, t) \leftarrow \Pi_{Ref-2}(s, t) \cup \{\rho_i\}, root \leftarrow \rho_i$
- 26:  $\Pi_{Ref-2}(s, t) \leftarrow \Pi_{Ref-2}(s, t) \cup \{t\}$
- 27: **return**  $\Pi_{Ref-2}(s, t)$

(i) *Binary search initial path finding*: Lines 6-15, see Figure 6 (a). In lines 6-9, we first have the blue ray  $\Pi_m = (s, m_1, R_1^m)$  that does not pass the whole  $S$ , we set  $[a_1, b_1] = [p_1, m_1]$ . In lines 10-15, we then have the purple ray  $\Pi_{m^1} = (s, m_1^1, m_2^1, R_2^m)$  passes the whole  $S$ , we set  $[a_1, b_1] = [m_1^1, m_1]$  and  $[a_2, b_2] = [m_2^1, q_2]$ .

(ii) *Effective weight pruning*: Lines 16-24. The purple ray passes the whole  $S$  for the first time, we can use effective weight pruning. In line 17 and Figure 6 (a), we get  $u$ . In lines 18-22 and Figure 6 (b), we (1) get  $u_p$  and  $f_{ef} = \Delta u_p p_1 q_1$ , (2) calculate  $w_{ef}$  using purple line  $sm_1^1$ , the orange dashed line  $m_1^1 u_p, f_1, f_{ef}, w_1$  and Snell's law, (3) get  $t_p$ , (4) set  $m_{ef}$  to be unknown and use Snell's law in vector form [1],

then build a quartic equation with unknown at the power of four using  $w_1$ ,  $w_{ef}$ , the dark blue line  $\overline{sm_{ef}}$  and the green dashed line  $\overline{m_{ef}t_p}$ , and use root formula [19] to solve  $m_{ef}$ . In lines 23-24 and Figure 6 (c), we compute the dark blue ray  $\Pi_{m^2} = (s, m_{ef}, m_2^2, R_2^{m^2})$ , and set  $[a_1, b_1] = [m_1^1, m_{ef}]$  and  $[a_2, b_2] = [m_2^1, m_2^2]$ .

(iii) *Binary search refined path finding*: Lines 2, 6-15, 25-26, see Figure 6 (d). In lines 6-15, we iterate until  $|a_1 b_1| = |m_1^1 m_{ef}| < \delta$ . In line 25, we have  $\rho_1$ , the pink dashed link  $\Pi_{Ref-2}(s, t) = (s, \rho_1)$ , and  $root = \rho_1$ . In line 2, we iterate to obtain the green ray  $\Pi_{m^3} = (\rho_1, m_3^2, R_2^{m^3})$  and the yellow ray  $\Pi_{m^4} = (\rho_1, m_4^2, R_2^{m^4})$ . Until we process all the edges in  $S = (e_1, e_2)$ , we get result path  $\Pi_{Ref-2}(s, t) = (s, \rho_1, \rho_2, t)$ .

3) *Error guaranteed path refinement*: See Figure 3 (h).

**Detail and example**: Algorithm 3 shows this step, and the following is an example.

---

**Algorithm 3** *ErrGuarRef* ( $s, t, SP_{Ref}, NodeInfo$ )

---

**Input**: source  $s$ , destination  $t$ , Steiner points  $SP_{Ref}$ , node information  $dist_{Roug}(u)$  and  $prev_{Roug}(u)$  (based on  $s$ ) for each  $u \in G_{Roug}.V$   
**Output**: the refined path  $\Pi_{Ref-3}(s, t)$   
1: build a weighted graph  $G_{Ref}$  using  $SP_{Ref}$ , enqueue  $\{s, 0\}$  into  $Q$   
2: **for** each  $u \in G_{Ref}.V$  **do**  
3:   **if**  $u \in G_{Ref}.V \setminus G_{Roug}.V$  (resp.  $u \in G_{Roug}.V$ ) **then**  
4:      $dist_{Ref}(u) \leftarrow \infty$  (resp.  $dist_{Roug}(u)$ )  
5:      $prev_{Ref}(u) \leftarrow NULL$  (resp.  $prev_{Roug}(u)$ )  
6: **while**  $Q$  is not empty and the to-be-dequeued node is not  $t$  **do**  
7:   dequeue node  $v$  from  $Q$  with smallest distance value  $dist_{Ref}(v)$   
8:   **for** each adjacent vertex  $v'$  of  $v$ , such that  $vv' \in G_{Ref}.E$  **do**  
9:     **if**  $dist_{Ref}(v') > dist_{Ref}(v) + w_{vv'} \cdot d(v, v')$  **then**  
10:        $dist_{Ref}(v') \leftarrow dist_{Ref}(v) + w_{vv'} \cdot d(v, v')$ ,  $prev_{Ref}(v') \leftarrow v$   
11:       enqueue  $\{v', dist_{Ref}(v')\}$  into  $Q$   
12:  $u \leftarrow prev_{Ref}(t)$ ,  $\Pi_{Ref-3}(s, t) \leftarrow \{t\}$   
13: **while**  $u \neq s$  **do**  
14:    $\Pi_{Ref-3}(s, t) \leftarrow \Pi_{Ref-3}(s, t) \cup \{u\}$ ,  $u \leftarrow prev_{Ref}(u)$   
15:  $\Pi_{Ref-3}(s, t) \leftarrow \Pi_{Ref-3}(s, t) \cup \{s\}$ , reverse  $\Pi_{Ref-3}(s, t)$   
16: **return**  $\Pi_{Ref-3}(s, t)$

---

(i) *Distance and previous node initialization*: Lines 2-5. For  $d$ ,  $dist_{Ref}(d) = \infty$  and  $prev_{Ref}(d) = NULL$ ; for  $b$ ,  $dist_{Ref}(b) = dist_{Roug}(b) = 9 + 1 \times 5 = 14$  and  $prev_{Ref}(b) = prev_{Roug}(b) = a$ .

(ii) *Priority queue looping*: Lines 6-11. Suppose  $Q$  stores  $\{\{a, 9\}, \{c, 8\}\}$ , we dequeue  $c$ . One adjacent node of  $c$  is  $b$ , since  $dist_{Ref}(b) = 14 < dist_{Ref}(c) + w_{bc} \cdot d(b, c) = 8 + 1 \times 7 = 15$ , there is no need to enqueue  $\{b, dist_{Ref}(b) = 15\}$  into  $Q$ .

(iii) *Path retrieving*: Lines 16-19. We obtain  $\Pi_{Ref-3}(s, t)$ .

### F. Theoretical Analysis

Theorem 1 shows the analysis of algorithm *Roug-Ref*.

**Theorem 1.** *The running time and memory usage for algorithm Roug-Ref is  $O(n \log n + l)$  and  $O(n + l)$ . It guarantees that  $|\Pi(s, t)| \leq (1 + \epsilon)|\Pi^*(s, t)|$ .*

*Proof Sketch.* (1) The *running time* contains (i)  $O(n \log n)$  for the rough path calculation due to Dijkstra's algorithm on  $G_{Roug}$  with  $n$  nodes, (ii)  $O(n \log n)$  for the full edge sequence conversion due to Dijkstra's algorithm, (iii)  $O(l)$  for the Snell's law path refinement due to  $l$  edges in  $S$  and  $O(1)$  time in finding the optimal intersection point on each edge, and (iv)  $O(n \log n)$  for the error guaranteed path refinement due

to Dijkstra's algorithm on  $G_{Ref}$  with  $n$  nodes and the node information. (2) The *memory usage* contains (i)  $O(n)$  for the rough path calculation, (ii)  $O(n)$  for the full edge sequence conversion, (iii)  $O(l)$  for the Snell's law path refinement, and (iv)  $O(n)$  for the error guaranteed path refinement. (3) The *error bound* is due to the rough path calculation in Section IV-A2, and the path checking and the error guaranteed path refinement in Section IV-A3. The detailed proof appears in the appendix.  $\square$

## V. EMPIRICAL STUDIES

### A. Experimental Setup

We conducted the experiments on a Linux machine with 2.67 GHz CPU and 48GB memory. All algorithms were implemented in C++. The experimental setup followed the setup used in previous studies [14], [15], [22], [30], [31].

**Datasets**: We conducted our experiment on 27 real terrain datasets in Table II, where *EP* has more mountains compared with the other 4 original datasets. For small-version and multi-resolution datasets, we generated them using *BH* and *EP* following the procedure in [22], [30], [31] (which creates a terrain surface with different resolutions). We use the slope of a face in terrain datasets as the weight of that face [13], due to the distinct face slope, each face has a distinct weight.

**Algorithms**: We compared *Roug-Ref* with  $(1 + \epsilon)$ -approximate algorithms, i.e., (1) *EdgSeq-Adp* [29], (2) the best-known algorithm *FixSP* [13], [18], (3) *FixSP-NoWei-Adp* [14], (4) *LogSP-Adp* [4], and (5) variations of *Roug-Ref*. We also compared with (1) *EdgSeq* [29] without error bound, (2 & 3) *LogSP* [4] and *Roug* with distance errors larger than  $(1 + \epsilon)$  in the appendix.

**Query Generation**: We randomly chose pairs of vertices in  $V$  as source and destination (the corresponding path has different distances and covers different faces with different weights), and we report the average, minimum, and maximum results of 100 queries.

**Factors and Measurements**: We studied three factors, namely (1)  $k$ , (2)  $\epsilon$ , and (3) dataset size (i.e., the number of faces in a terrain surface). We used five measurements to evaluate the algorithm performance, namely (1) *query time*, (2) *memory usage*, (3) *chances of using error guaranteed path refinement step*, (4) *average number of Steiner points per edge (used in path calculation)*, and (5) *distance error* (we use *EdgSeq-Adp* with  $\epsilon = 0.05$  to simulate the exact result since no algorithm can solve the weighted region problem exactly).

### B. Experimental Results

We compared (1) all algorithms on datasets with less than 250k faces, and (2) algorithms not involving *FixSP* components on datasets with more than 250k faces due to the expensive running time. The vertical bar means the minimum and maximum results.

1) *Ablation study of Roug-Ref*: In our algorithm *Roug-Ref*, we have 4 variations: (i) we do not use our efficient Steiner points placement scheme, i.e., we use algorithm *FixSP* for Steiner point placement, (ii) we remove the full edge



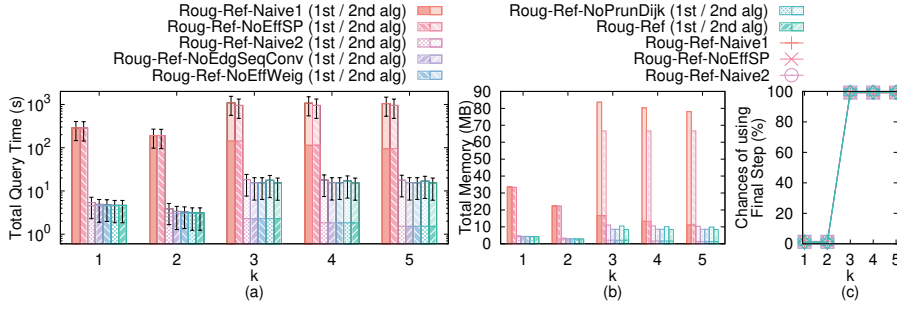


Fig. 7. Ablation study (effect of  $k$  on  $BH$ -small dataset)

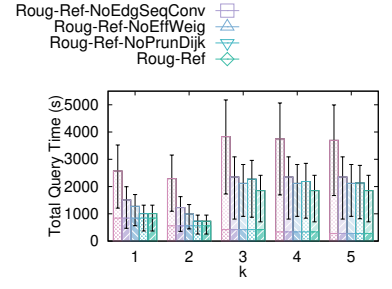


Fig. 8. Ablation study (effect of  $k$  on  $BH$  dataset)

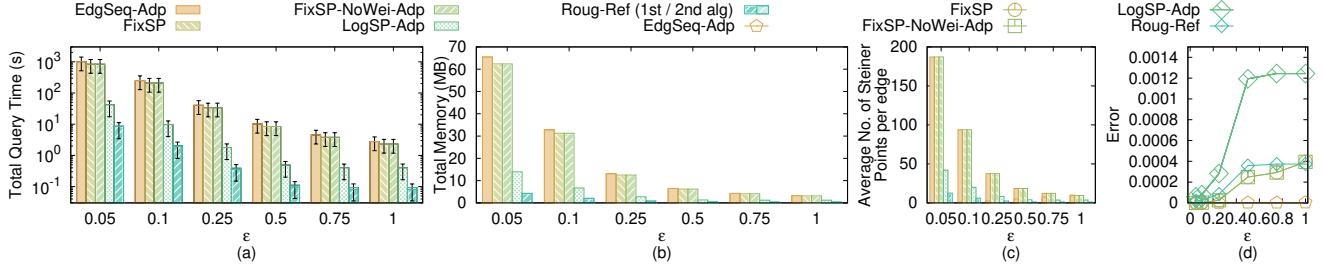


Fig. 9. Baseline comparisons (effect of  $\epsilon$  on  $EP$ -small dataset)

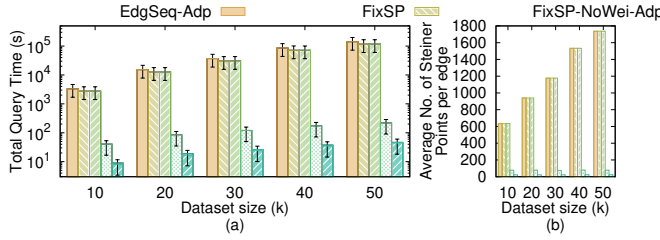


Fig. 10. Baseline comparisons (effect of dataset size on multi-resolution of  $EP$ -small datasets)

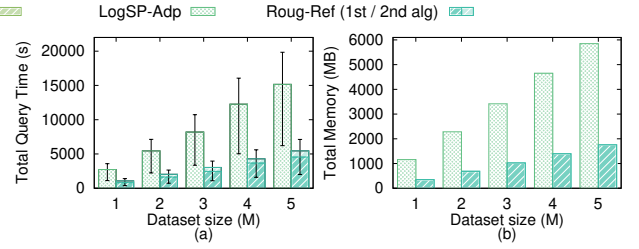


Fig. 11. Scalability test

sequence conversion step, (iii) we remove the effective weight pruning out sub-step in the Snell's law path refinement step, and (iv) we do not use the node information for pruning in the error guaranteed path refinement step, for ablation study (they correspond to four techniques in Section IV-C). We use (i) *Roug-Ref-NoEffSP*, (ii) *Roug-Ref-NoEdgSeqConv*, (iii) *Roug-Ref-NoEffWeig*, and (iv) *Roug-Ref-NoPrunDijk*, to denote these variations. If we do not use the rough-refine concept, *Roug-Ref* becomes *LogSP-Adp*. We adapt *FixSP*, *FixSP-NoWei-Adp* and *EdgSeq-Adp* (resp. *LogSP-Adp*) by using our rough-refine concept, and denote it as *Roug-Ref-Naive1* (resp. *Roug-Ref-Naive2*). Since  $k$  will only affect the variations of *Roug-Ref* and our algorithm *Roug-Ref*, we study the effect of  $k$  here.

**Effect of  $k$ :** In Figure 7 (resp. Figure 8), we tested 5 values of  $k$  from  $\{1, 2, 3, 4, 5\}$  on  $BH$ -small (resp.  $BH$ ) dataset by setting  $\epsilon$  to be 0.1 (resp. 0.25) for ablation study (i) When  $k \leq 2$  and  $k$  increases, more Steiner points are removed and *Roug* runs faster, so the query time and memory usage of these algorithms decreases. But when  $k > 2$ , it has a higher chance (more than 99%) that *Ref* needs to perform the error guaranteed path refinement step, so the query time and memory usage have a sudden increase. Thus, the optimal  $k$  is

2 (also verified on other datasets shown in the appendix). (ii) When  $k = 2$ , the query time of *Roug-Ref-Naive1* and *Roug-Ref-NoEffSP* are 230s and 210s on  $BH$ -small dataset, but their difference is small due to the log-scale in Figure 7 (a). Due to the same reason, the difference in query time of the other four algorithms on  $BH$ -small dataset is also small, so we compare them with linear-scale in Figure 8 (which shows the usefulness of each component).

**2) Baseline comparisons:** We then study the effect of  $\epsilon$  and dataset size on other baselines when  $k = 2$ .

**Effect of  $\epsilon$ :** In Figure 9, we tested 6 values of  $\epsilon$  from  $\{0.05, 0.1, 0.25, 0.5, 0.75, 1\}$  on  $EP$ -small dataset. (i) When  $\epsilon$  increases, fewer Steiner points are required so the query time and memory usage decrease. (ii) The query time and memory usage of *Ref* is much smaller than that of *Roug*. (iii) *Roug-Ref* performs better than all other algorithms in terms of query time and memory usage, and it is clearer to observe the superior performance of *Roug-Ref*, due to the rough-refine concept and four novel techniques. The distance error of all algorithms is very small, the value is 0.0004 when  $\epsilon = 1$  for *Roug-Ref*. (iv) When  $\epsilon = 0.05$ , *Roug-Ref* has 160 fewer Steiner points per edge than *FixSP* and *FixSP-NoWei-Adp*, the

query time and calculated path's distance of *Roug-Ref* is 14.6s and 105.3m, but are both  $23,800s \approx 7.2$  hours and 105.2m for *FixSP* and *FixSP-NoWei-Adp*, since *Roug-Ref* uses the rough-refine concept. *EdgSeq-Adp* performs worse than *FixSP* since *EdgSeq-Adp* first uses *FixSP* and then uses Snell's law for the weighted shortest path calculation. *LogSP-Adp* does not perform well since it does not utilize Snell's law.

**Effect of dataset size:** In Figure 10, we tested 5 values of dataset size from  $\{10k, 20k, 30k, 40k, 50k\}$  on multi-resolution of *EP-small* datasets by setting  $\epsilon$  to be 0.1. When the dataset size is 50k, *Roug-Ref*'s query time is  $10^3$  times,  $10^3$  times,  $10^3$  times and 6 times smaller than that of *EdgSeq-Adp*, *FixSP*, *FixSP-NoWei-Adp* and *LogSP-Adp*, respectively.

3) **Scalability test:** In Figure 11, we tested 5 values of dataset size from  $\{1M, 2M, 3M, 4M, 5M\}$  on multi-resolution of *EP* datasets by setting  $\epsilon$  to be 0.25. When the dataset size is 5M, *Roug-Ref*'s query time is still reasonable. However, the query times for *EdgSeq-Adp*, *FixSP* and *FixSP-NoWei-Adp* are larger than 7 days, so they are excluded from the figure.

4) **Other algorithms comparisons:** Given  $\epsilon$ , *Roug-Ref* can calculate a path with distance  $d$ . But, *EdgSeq* does not have error bound, *LogSP* and *Roug* have distance errors larger than  $(1 + \epsilon)$ . We finetune their input to make their calculated path also with distance  $d$ . When  $\epsilon = 0.1$ , *Roug-Ref*, *EdgSeq*, *LogSP* and *Roug* run in 3s, 140s, 113s and 110s on *BH-small* dataset.

5) **Case study:** We conducted a case study on the earthquake recuse in Section I-A. The rescue team can walk (resp. drive cars) with an average speed of 3km/h (resp. 90km/h) to pass through the destroyed (resp. non-destroyed) region. In Figure 1 (b), the unweighted (resp. weighted) shortest path has a distance of 4.3km (resp. 4.6km). So, the recuse time of using the unweighted (resp. weighted) shortest path is 1.4 hours  $\approx \frac{4.3km}{3km/h}$  (resp. 3 min  $\approx \frac{4.6km}{90km/h} \times 60min/h$ ). The query time for the best-known algorithm *FixSP* and *Roug-Ref* are 11,900s  $\approx 3.3$  hours and 7.3s. So, the weighted shortest path calculated by *Roug-Ref* is the best path for recuse.

6) **Summary:** *Roug-Ref* is up to 1630 times and 40 times better than the best-known algorithm *FixSP* in terms of running time and memory usage. When the dataset size is 50k with  $\epsilon = 0.1$ , *Roug-Ref*'s running time is 73s  $\approx 1.2$  min, and memory usage is 43MB, but *FixSP*'s running time is 119,000s  $\approx 1.5$  days, and memory usage is 2.9GB. The user study confirms that *Roug-Ref* is the optimal algorithm in earthquake recuse.

## VI. CONCLUSION

We propose a two-step  $(1 + \epsilon)$ -approximate algorithm *Roug-Ref* for solving the 3D weighted region problem. Future work can be introducing a new pruning step (by considering other geometric information of the weighted terrain surface) to further reduce the algorithm's running time.

## REFERENCES

- [1] "Snell's law in vector form," 2023. [Online]. Available: <https://physics.stackexchange.com/questions/435512/snells-law-in-vector-form>
- [2] "Japan earthquake death toll reaches 206 as government includes indirect deaths," 2024. [Online]. Available: <https://www.accuweather.com/en/weather-news/japan-earthquake-death-toll-reaches-206-as-government-includes-indirect-deaths/1611292>
- [3] "Moderate mag. 4.1 earthquake - 6.3 km north-east of sierre, valais, switzerland," 2024. [Online]. Available: <https://www.volcanodiscovery.com/earthquakes/quake-info/1451397/mag4quake-Oct-24-2016-Leukerbad-VS.html>
- [4] L. Aleksandrov, M. Lanthier, A. Maheshwari, and J.-R. Sack, "An  $\epsilon$ -approximation algorithm for weighted shortest paths on polyhedral surfaces," in *Workshop on Algorithm Theory*. Springer, 1998.
- [5] C. Amante and B. W. Eakins, "Etopo1 arc-minute global relief model: procedures, data sources and analysis," 2009.
- [6] C. Bassem, S. Honcharuk, and M. Mokbel, "Route recommendation to facilitate carpooling," in *MDM*. IEEE, 2022, pp. 29–34.
- [7] C. Bueger, T. Liebetrau, and J. Franken, "Security threats to undersea communications cables and infrastructure—consequences for the eu," *Report for SEDE Committee of the European Parliament, PE702*, vol. 557, 2022.
- [8] J. Chen and Y. Han, "Shortest paths on a polyhedron," in *SOCG*, New York, NY, USA, 1990, p. 360–369.
- [9] M. Chen, R. A. Chowdhury, V. Ramachandran, D. L. Roche, and L. Tong, "Priority queues and dijkstra's algorithm," 2007.
- [10] J.-L. De Carufel, C. Grimm, A. Maheshwari, M. Owen, and M. Smid, "A note on the unsolvability of the weighted region shortest path problem," *Computational Geometry*, vol. 47, no. 7, pp. 724–727, 2014.
- [11] K. Deng, X. Zhou, H. T. Shen, Q. Liu, K. Xu, and X. Lin, "A multi-resolution surface distance model for k-nn query processing," *VLDBJ*, vol. 17, no. 5, pp. 1101–1119, 2008.
- [12] E. W. Dijkstra, "A note on two problems in connexion with graphs," *Numerische mathematik*, vol. 1, no. 1, pp. 269–271, 1959.
- [13] B. Huang, V. J. Wei, R. C.-W. Wong, and B. Tang, "Ear-oracle: on efficient indexing for distance queries between arbitrary points on terrain surface," *SIGMOD*, vol. 1, no. 1, pp. 1–26, 2023.
- [14] M. Kaul, R. C.-W. Wong, and C. S. Jensen, "New lower and upper bounds for shortest distance queries on terrains," *VLDB*, vol. 9, no. 3, pp. 168–179, 2015.
- [15] M. Kaul, R. C.-W. Wong, B. Yang, and C. S. Jensen, "Finding shortest paths on terrains by killing two birds with one stone," *VLDB*, vol. 7, no. 1, pp. 73–84, 2013.
- [16] J. Kim, "Submarine cables: the invisible fiber link enabling the internet," 2022. [Online]. Available: <https://dgtlinfra.com/submarine-cables-fiber-link-internet/>
- [17] M. Lanthier, "Shortest path problems on polyhedral surfaces." Ph.D. dissertation, Carleton University, 2000.
- [18] M. Lanthier, A. Maheshwari, and J.-R. Sack, "Approximating shortest paths on weighted polyhedral surfaces," *Algorithmica*, vol. 30, no. 4, pp. 527–562, 2001.
- [19] S. H. Lee, S. M. Im, and I. S. Hwang, "Quartic functional equations," *Journal of Mathematical Analysis and Applications*, vol. 307, no. 2, pp. 387–394, 2005.
- [20] H. Li and Z. Huang, "82 die in sichuan quake, rescuers race against time to save lives," 2024. [Online]. Available: <https://www.chinadailyhk.com/article/289413#82-die-in-Sichuan-quake-rescuers-race-against-time-to-save-lives>
- [21] J.-F. Libert and G. Waterworth, "13 - cable technology," in *Undersea Fiber Communication Systems (Second Edition)*. Academic Press, 2016, pp. 465–508.
- [22] L. Liu and R. C.-W. Wong, "Finding shortest path on land surface," in *SIGMOD*, 2011, pp. 433–444.
- [23] B. Max and W. Emil, "Principles of optics," 1959.
- [24] J. S. Mitchell and C. H. Papadimitriou, "The weighted region problem: finding shortest paths through a weighted planar subdivision," *Journal of the ACM (JACM)*, vol. 38, no. 1, pp. 18–73, 1991.
- [25] J. E. Nichol, A. Shaker, and M.-S. Wong, "Application of high-resolution stereo satellite images to detailed landslide hazard assessment," *Geomorphology*, vol. 76, no. 1–2, pp. 68–75, 2006.
- [26] C. Shahabi, L.-A. Tang, and S. Xing, "Indexing land surface for efficient knn query," *VLDB*, vol. 1, no. 1, pp. 1020–1031, 2008.
- [27] A. Suppasri, K. Pakoksung, I. Charvet, C. T. Chua, N. Takahashi, T. Ornthammarath, P. Latcharote, N. Leelawat, and F. Imamura, "Load-resistance analysis: an alternative approach to tsunami damage assessment applied to the 2011 great east japan tsunami," *Natural Hazards and Earth System Sciences*, vol. 19, no. 8, pp. 1807–1822, 2019.
- [28] X. Teng, G. Trajcevski, J.-S. Kim, and A. Züfle, "Semantically diverse path search," in *MDM*. IEEE, 2020, pp. 69–78.
- [29] N. Tran, M. J. Dinneen, and S. Linz, "Close weighted shortest paths on 3d terrain surfaces," in *SIGSPATIAL*, 2020, pp. 597–607.

- [30] V. J. Wei, R. C.-W. Wong, C. Long, and D. M. Mount, “Distance oracle on terrain surface,” in *SIGMOD*, 2017, pp. 1211–1226.
- [31] V. J. Wei, R. C.-W. Wong, C. Long, D. M. Mount, and H. Samet, “Proximity queries on terrain surface,” *TODS*, 2022.
- [32] S. Xing, C. Shahabi, and B. Pan, “Continuous monitoring of nearest neighbors on land surface,” *VLDB*, vol. 2, no. 1, pp. 1114–1125, 2009.
- [33] Y. Yan and R. C.-W. Wong, “Path advisor: a multi-functional campus map tool for shortest path,” *VLDB*, vol. 14, no. 12, pp. 2683–2686, 2021.

## APPENDIX A MOTIVATION

We give another motivation for our study.

**Cable placement:** Nowadays, over  $1.35 \times 10^5$  km of undersea optical fiber cable have been deployed on the seabed (represented as a weighted terrain surface) [16]. We want to minimize the weighted distance of the cable for cost saving. Deeper sea levels result in higher hydraulic pressure, which reduces the cable’s lifespan and increases repair and maintenance costs [7]. We assign larger weights to the terrain faces representing deeper sea levels. So, we can avoid placing the cable in these regions and reduce costs. In Figure 12, the weighted shortest path in blue line (resp. unweighted shortest path in purple dashed line) is routed in the regions with shallower (resp. deeper) sea levels. Our case study shows that the estimated cost of the cable following the weighted (resp. unweighted) shortest path is USD \$45.8M (resp. \$54.8M), which shows the usefulness of finding the weighted shortest path. Since we only need to calculate each path once, there is no need to pre-compute it. But, due to the large terrain datasets with more than 100M faces (e.g., for the cable between the US and China, the cable needs to pass through the whole seabed of the Pacific Ocean, which is a very large region), we need to efficiently calculate the path.

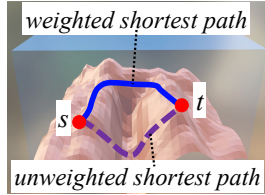


Fig. 12. Blue weighted and purple dashed unweighted shortest paths in cable placement

## APPENDIX B SUMMARY OF FREQUENT USED NOTATIONS

Table III shows a summary of frequent used notations.

## APPENDIX C EXAMPLE ON THE GOOD PERFORMANCE OF THE EFFECTIVE WEIGHT PRUNING SUB-STEP IN THE SNELL’S LAW PATH REFMENT STEP OF ALGORITHM *Ref*

We use a 1D example to illustrate why the effective weight pruning sub-step in the Snell’s law path refinement step of algorithm *Ref* can prune out unnecessary checking. Let 0 and 100 to be the position of the two endpoints of  $e_1$ , and we have  $[a_1 b_1] = [0, 100]$ . Assume that the position of the optimal intersection point  $r_1$  on the first edge is 87.32. Then, without

TABLE III  
SUMMARY OF FREQUENT USED NOTATIONS

| Notation                             | Meaning   |
|--------------------------------------|---|
| $T$                                  | The weighted terrain surface  |
| $V/E/F$                              | The set of vertices / edges / faces of $T$  |
| $n$                                  | The number of vertices of $T$   |
| $L$                                  | The length of the longest edge in $T$   |
| $N$                                  | The smallest integer value which is larger than or equal to the coordinate value of any vertex                  |
| $W/w$                                | The maximum / minimum weights of $T$  |
| $h$                                  | The minimum height of any face in $F$   |
| $\epsilon$                           | The error parameter   |
| $\eta$                               | The constant calculated using the remaining Steiner points for controlling the error                            |
| $k$                                  | The removing value  |
| $\Pi^*(s, t)$                        | The optimal weighted shortest path  |
| $r_i$                                | The intersection point of $\Pi^*(s, t)$ and an edge in $E$  |
| $\Pi(s, t)$                          | The final calculated weighted shortest path   |
| $ \Pi(s, t) $                        | The weighted distance of $\Pi(s, t)$  |
| $\overline{pq}$                      | A line between two points $p$ and $q$ on a face   |
| $\Pi_{Roug}(s, t)$                   | The rough path calculated using algorithm <i>Roug</i>   |
| $\Pi_{Ref-1}(s, t)$                  | The modified rough path calculated using the full edge sequence conversion step of algorithm <i>Ref</i>         |
| $\Pi_{Ref-2}(s, t)$                  | The refined path calculated using the Snell’s law path refinement step of algorithm <i>Ref</i>                  |
| $\Pi_{Ref-3}(s, t)$                  | The refined path calculated using the error guaranteed path refinement step of algorithm <i>Ref</i>             |
| $\rho_i$                             | The intersection point of $\Pi_{Ref-2}(s, t)$ and an edge in $E$  |
| $\xi$                                | The iteration counts of single endpoint cases in the full edge sequence conversion step of algorithm <i>Ref</i> |
| $S$                                  | The edge sequence that $\Pi_{Ref-1}(s, t)$ connects from $s$ to $t$ in order based on $T$                       |
| $l$                                  | The number of edges in $S$  |
| $\Pi_c$                              | A 3D surface Snell’s ray  |
| $SP_{Roug} / SP_{Ref}$               | The set of Steiner points on each edge of $E$ used in algorithm <i>Roug</i> / <i>Ref</i>                        |
| $G_{Roug} / G_{Ref}$                 | The connected weighted graph used in algorithm <i>Roug</i> / <i>Ref</i>   |
| $G_{Roug} \cdot V / G_{Ref} \cdot V$ | The set of vertices in the connected weighted graph used in algorithm <i>Roug</i> / <i>Ref</i>                  |
| $G_{Roug} \cdot E / G_{Ref} \cdot E$ | The set of edges in the connected weighted graph used in algorithm <i>Roug</i> / <i>Ref</i>                     |

the effective weight pruning sub-step in the Snell’s law path refinement step of algorithm *Ref*, the searching interval will be  $[50, 100]$ ,  $[75, 100]$ ,  $[75, 87.5]$ ,  $[81.25, 87.5]$ ,  $[84.375, 87.5]$ ,  $[85.9375, 87.5]$ ,  $[86.71875, 87.5]$ ,  $[87.109375, 87.5] \dots$ . But, with the effective weight pruning sub-step in the Snell’s law path refinement step of algorithm *Ref*, assume that we still need to use several iterations of the original binary search to let  $\Pi_m$  pass the whole  $S$  based on  $T$ , and we need to check  $[50, 100]$ ,  $[75, 100]$ ,  $[75, 87.5]$ . After checking the interval  $[75, 87.5]$ , we get a  $\Pi_m$  that passes the whole  $S$  based on  $T$ . Assume we calculate  $m_{ef}$  as 87 using effective weight pruning step. As a result, in the next checking, we can directly limit the searching interval to be  $[87, 87.5]$ , which can prune out some unnecessary interval checking including  $[81.25, 87.5]$ ,  $[84.375, 87.5]$ ,  $[85.9375, 87.5]$ ,  $[86.71875, 87.5]$ , and thus, the effective weight pruning sub-step in the Snell’s law path refinement step of algorithm *Ref* can save the running time and memory usage.

### A. Experimental Results

(1) Figure 13 and Figure 14, (2) Figure 15 and Figure 16 show the result on the *BH-small* dataset when varying  $k$  and  $\epsilon$ , respectively. (3) Figure 17 and Figure 18, (4) Figure 19 and Figure 20 show the result on the *BH* dataset when varying  $k$  and  $\epsilon$ , respectively. (5) Figure 21 and Figure 22, (6) Figure 9 and Figure 23 show the result on the *EP-small* dataset when varying  $k$  and  $\epsilon$ , respectively. (7) Figure 24 and Figure 25, (8) Figure 26 and Figure 27 show the result on the *EP-small* dataset when varying  $k$  and  $\epsilon$ , respectively. (9) Figure 28 and Figure 29 show the result on multi-resolution of *BH-small* datasets when varying dataset size. (10) Figure 30 and Figure 31 show the result on multi-resolution of *BH* datasets when varying dataset size. (11) Figure 32 and Figure 33 show the result on multi-resolution of *EP-small* datasets when varying dataset size. (12) Figure 34 and Figure 35 show the result on multi-resolution of *EP* datasets when varying dataset size.

1) **Ablation study of *Roug-Ref*:** In our algorithm *Roug-Ref*, recall that we have six variations of algorithms, i.e., (1) *Roug-Ref-NoEffSP*, (2) *Roug-Ref-NoEdgSeqConv*, (3) *Roug-Ref-NoEffWeig*, (4) *Roug-Ref-NoPrunDijk*, (5) *Roug-Ref-Naive1*, and (6) *Roug-Ref-Naive2*, for ablation study. Since  $k$  will only affect the variations of *Roug-Ref* and our algorithm *Roug-Ref*, we study the effect of  $k$  in this subsection.

**Effect of  $k$ .** In Figure 13, Figure 17, Figure 21 and Figure 24, we tested 5 values of  $k$  from  $\{1, 2, 3, 4, 5\}$  on *BH-small*, *BH*, *EP-small* and *EP* datasets by setting  $\epsilon$  to be 0.1 on *BH-small* and *EP-small* datasets, and 0.25 on *BH* and *EP* datasets. Figure 14, Figure 18, Figure 22 and Figure 25 are the separated query time, memory usage, and the average number of Steiner points per edge in two steps for these results.

(i) When  $k \leq 2$  and  $k$  increases, more Steiner points are removed and *Roug* runs faster, so the query time and memory usage of these algorithms decreases. But when  $k > 2$ , it has a higher chance (more than 99%) that *Ref* needs to perform the error guaranteed path refinement step, so the query time and memory usage have a sudden increase. Thus, the optimal  $k$  is 2 (also verified on other datasets). (ii) When  $k = 2$ , the query time of *Roug-Ref-Naive1* and *Roug-Ref-NoEffSP* are 230s and 210s on *BH-small* dataset, but their difference is small due to the log-scale in Figure 7 (a). Due to the same reason, the difference in query time of the other four algorithms on *BH-small* dataset is also small, so we compare them with linear-scale in Figure 8 (which shows the usefulness of each component).

2) **Baseline comparisons:** From the previous subsection, *Roug-Ref* is the best algorithm among different variations. Starting from this subsection, we study the effect of  $\epsilon$  and the dataset size by comparing different baselines with *Roug-Ref* when  $k = 2$ . But, they will not affect the chance of using error guaranteed path refinement step in *Roug-Ref*, and the

chance is always smaller than 1% when  $k = 2$ , so we omit it in the following comparisons.

**Effect of  $\epsilon$ .** In Figure 15, Figure 19, Figure 9 and Figure 26, we tested 6 values of  $\epsilon$  from  $\{0.05, 0.1, 0.25, 0.5, 0.75, 1\}$  on *BH-small*, *BH*, *EP-small* and *EP* datasets by setting  $k$  to be 2. Figure 16, Figure 20, Figure 23 and Figure 27 are the separated query time and memory usage in two steps for these results. Since when  $k = 2$ , there is no need to place Steiner points in *Ref* (i.e., all Steiner points are used in *Roug*), so there is no need to show the separated average number of Steiner points per edge in two steps. (i) When  $\epsilon$  increases, fewer Steiner points are required so the query time and memory usage decrease. (ii) The query time and memory usage of *Ref* is much smaller than that of *Roug*. (iii) *Roug-Ref* performs better than all other algorithms in terms of query time and memory usage, and it is clearer to observe the superior performance of *Roug-Ref*, due to the rough-refine concept and four novel techniques. The distance error of all algorithms is very small, the value is 0.0004 when  $\epsilon = 1$  for *Roug-Ref*. (iv) When  $\epsilon = 0.05$ , *Roug-Ref* has 160 fewer Steiner points per edge than *FixSP* and *FixSP-NoWei-Adp*, the query time and calculated path's distance of *Roug-Ref* is 14.6s and 105.3m, but are both 23,800s  $\approx$  7.2 hours and 105.2m for *FixSP* and *FixSP-NoWei-Adp*, since *Roug-Ref* uses the rough-refine concept. *EdgSeq-Adp* performs worse than *FixSP* since *EdgSeq-Adp* first uses *FixSP* and then uses Snell's law for the weighted shortest path calculation. *LogSP-Adp* does not perform well since it does not utilize Snell's law.

**Effect of dataset size:** In Figure 28 and Figure 32, we tested 5 values of dataset size from  $\{10k, 20k, 30k, 40k, 50k\}$  on multi-resolution of *BH-small* AND *EP-small* datasets by setting  $\epsilon$  to be 0.1 and  $k$  to be 2. Figure 29 and Figure 33 are the separated query time and memory usage in two steps for these results. Since when  $k = 2$ , there is no need to place Steiner points in *Ref* (i.e., all Steiner points are used in *Roug*), so there is no need to show the separated average number of Steiner points per edge in two steps. *Roug-Ref* performs better than *FixSP*, *FixSP-NoWei-Adp* and *LogSP*. (1) When the dataset size increases, the query time and the average number of Steiner points per edge of all algorithms increase. (2) *Roug-Ref* has the smallest query time. When the dataset size is 50k, *Roug-Ref*'s query time is  $10^3$  times,  $10^3$  times,  $10^3$  times and 6 times smaller than that of *EdgSeq-Adp*, *FixSP*, *FixSP-NoWei-Adp* and *LogSP-Adp*, respectively.

3) **Scalability test:** In Figure 30 and Figure 34, we tested 5 values of dataset size from  $\{1M, 2M, 3M, 4M, 5M\}$  on multi-resolution of *BH* and *EP* datasets by setting  $\epsilon$  to be 0.25 and  $k$  to be 2. Figure 31 and Figure 35 are the separated query time and memory usage in two steps for these results. Since when  $k = 2$ , there is no need to place Steiner points in *Ref* (i.e., all Steiner points are used in *Roug*), so there is no need to show the separated average number of Steiner points per edge in two steps. (i) *Roug-Ref* can still beat *LogSP-Adp* in terms of the query time and memory usage. (ii) When the dataset size is 5M, *Roug-Ref*'s query time is still reasonable. However, the query times for *EdgSeq-Adp*, *FixSP* and *FixSP-NoWei-Adp* are



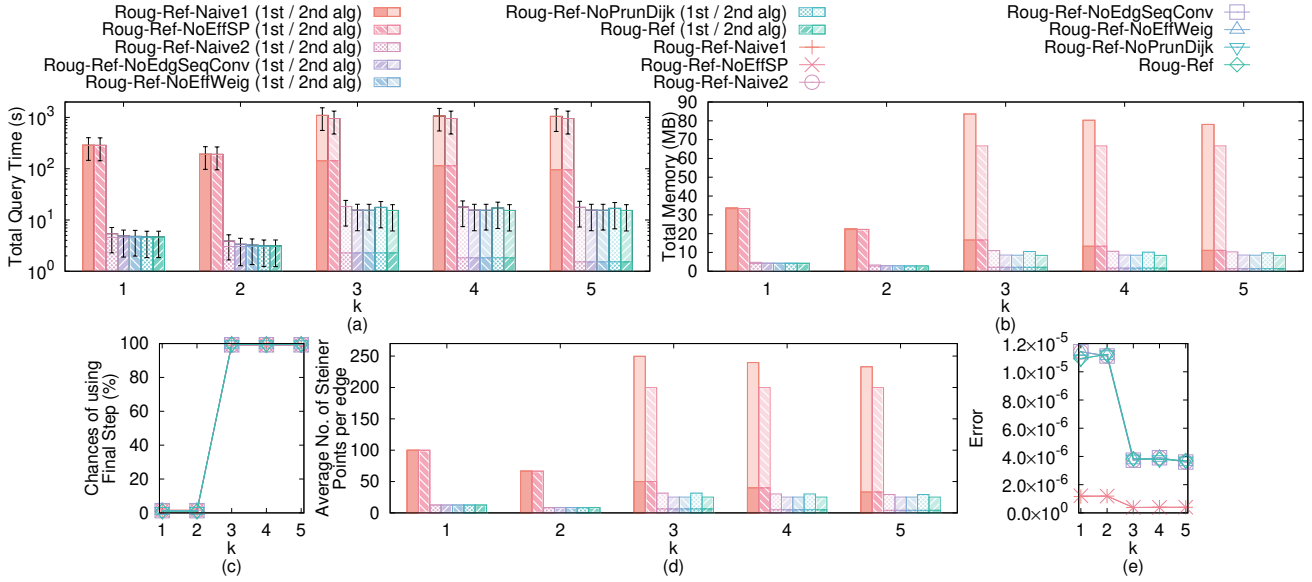


Fig. 13. Ablation study (effect of  $k$  on *BH-small* dataset)

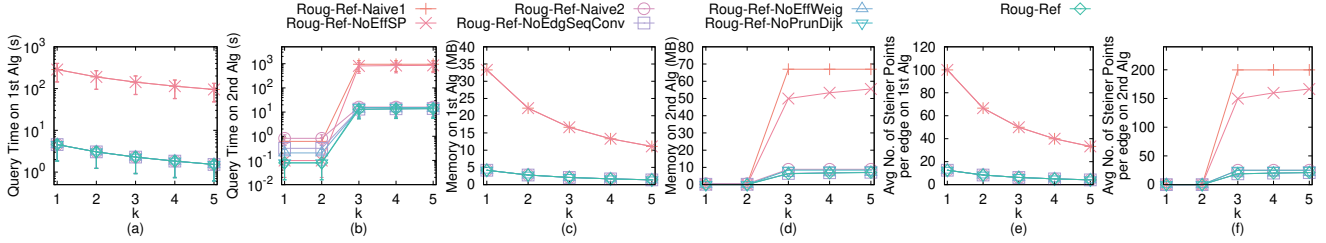


Fig. 14. Ablation study (effect of  $k$  on *BH-small* dataset with separated query time, memory usage, and the average number of Steiner points per edge in two steps)

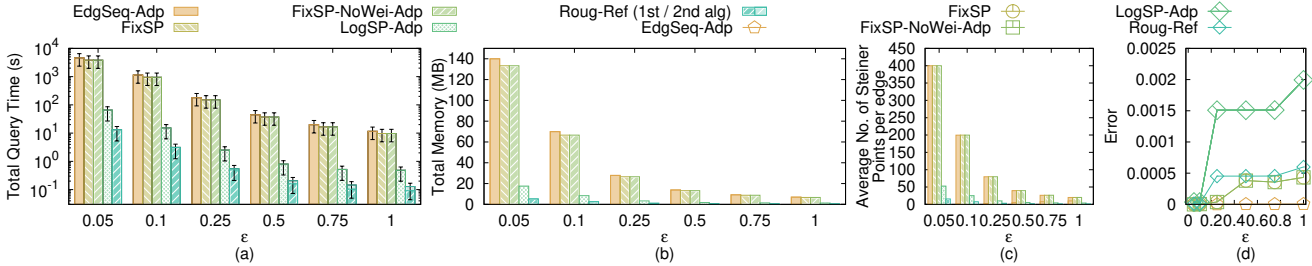


Fig. 15. Baseline comparisons (effect of  $\epsilon$  on *BH-small* dataset)

larger than 7 days, so they are excluded from the figure.

4) **Other algorithms comparisons:** In Figure 36 and Figure 37, we compare *EdgSeq*, *LogSP* and *Roug* with *Roug-Ref* using the method mentioned in Section V-B4. *Roug-Ref*, *EdgSeq*, *LogSP* and *Roug* run in 3s, 140s, 113s and 110s when  $\epsilon = 0.1$  on *BH-small* dataset due to the rough-refine concept in *Roug-Ref*.

5) **Case study (earthquake and avalanche):** Figure 38 and Figure 39 show the result for the earthquake and avalanche recuse case study when varying  $\epsilon$ . Our motivation and user study has already shown that the weighted shortest path is better than the unweighted shortest path due to the small recuse time. When  $\epsilon = 0.05$ , the average query time for

the state-of-the-art algorithm *FixSP* and our algorithm *Roug-Ref* are 11,900s  $\approx$  3.3 hours and 7.3s, respectively. So, the weighted shortest path calculated by *Roug-Ref* is the most suitable algorithm for earthquake and avalanche recuse.

6) **Case study (Path Advisor):** We conducted a case study on *Path Advisor* [33] as mentioned in Section I-A by using *PA* dataset [33]. We chose two places in *Path Advisor* as source and destination, and repeated it for 100 times to calculate the path (with  $\epsilon = 0.5$ ). In Figure 1 (c), the weighted (resp. unweighted) shortest path has distance 105.8m (resp. 98.4m). We presented the figure and the path distance result to 30 users (i.e., university students), and 96.7% of users think the blue path is the more realistic since it maintains a safe distance

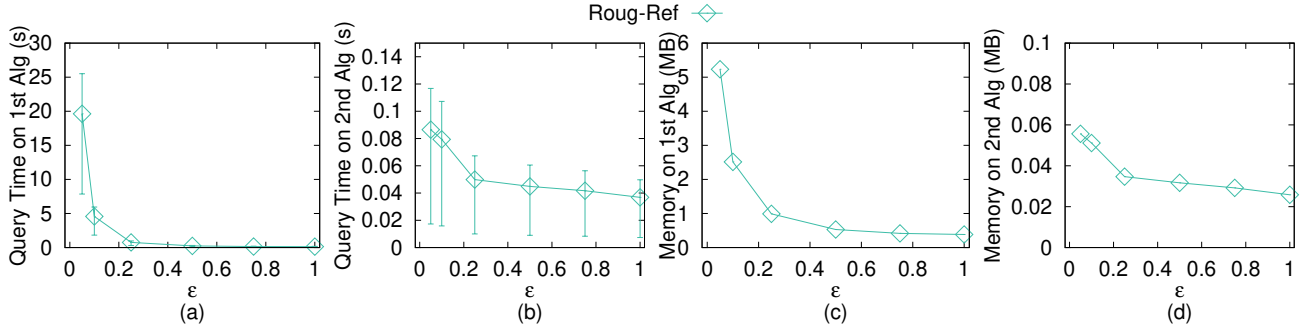


Fig. 16. Baseline comparisons (effect of  $\epsilon$  on *BH-small* dataset with separated query time and memory usage in two steps)

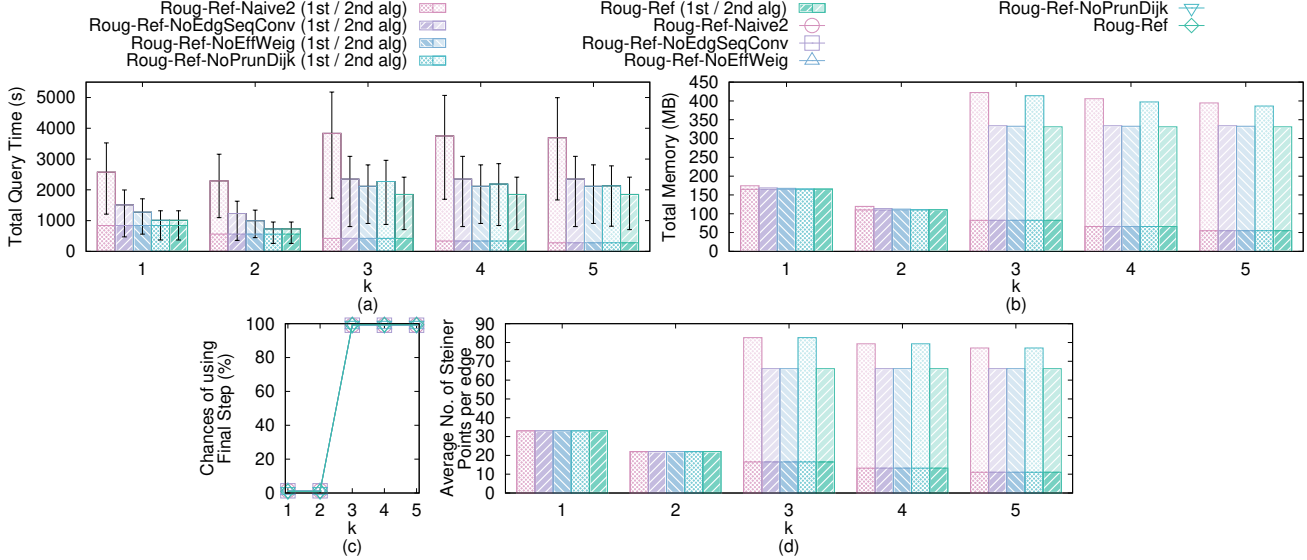


Fig. 17. Ablation study (effect of  $k$  on *BH* dataset)

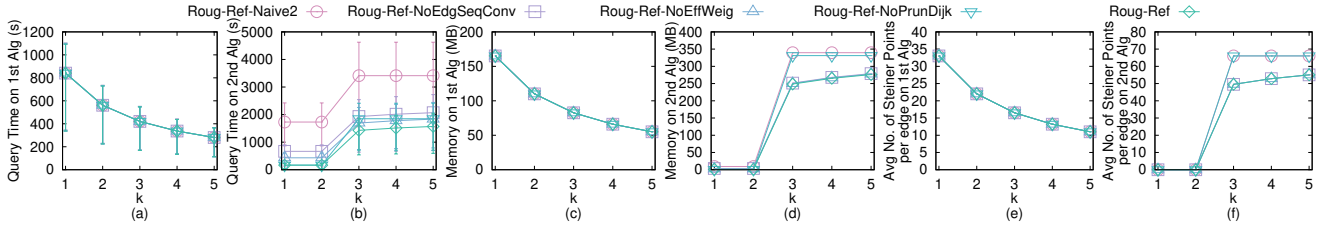


Fig. 18. Ablation study (effect of  $k$  on *BH* dataset with separated query time, memory usage, and the average number of Steiner points per edge in two steps)

from obstacles and avoids abrupt changes in direction. The average query time for the best-known algorithm *FixSP* and *Roug-Ref* are 16.62s and 0.1s, respectively.

Figure 40 and Figure 41 show the result for Path Advisor user study when varying  $\epsilon$ . When  $\epsilon = 0.5$ , the average query time for the state-of-the-art algorithm *FixSP* and our algorithm *Roug-Ref* are 16.62s and 0.1s, respectively. In addition, in a map application, the query time is the most crucial factor since users would like to get the result in a shorter time. Thus, *Roug-Ref* is the most suitable algorithm for Path Advisor.

**7) Case study (cable placement):** We conducted a case study on the cable placement as mentioned in Section A by using *SB* dataset [5]. The average life expectancy of a cable is

25 years [21], and if the cable is in deep waters (e.g., 8.5km or greater), the cable needs to be repaired frequently (e.g., its life expectancy is reduced to 20 years) [21]. We randomly chose pairs of points as source and destination, respectively, and repeated it 100 times to calculate the path (with  $\epsilon = 0.5$ ). In Figure 12, the weighted (resp. unweighted) shortest path has distance 457.9km (resp. 438.3km). Given the cost of undersea cable, i.e., USD \$25,000/km [16], when constructing a cable that will be used for 100 years [21], the total estimated cost for the blue and dashed purple paths are USD \$45.8M ( $= \frac{100\text{years}}{25\text{years}} \times 457.9\text{km} \times \$25,000/\text{km}$ ) and \$54.8M ( $= \frac{100\text{years}}{20\text{years}} \times 438.3\text{km} \times \$25,000/\text{km}$ ), respectively. The average query time for the best-known algorithm *FixSP* and *Roug-Ref* are 22.50s

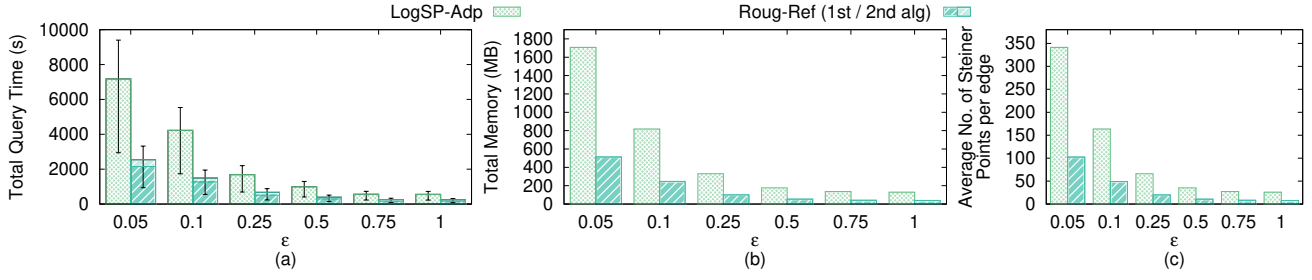


Fig. 19. Baseline comparisons (effect of  $\epsilon$  on *BH* dataset)

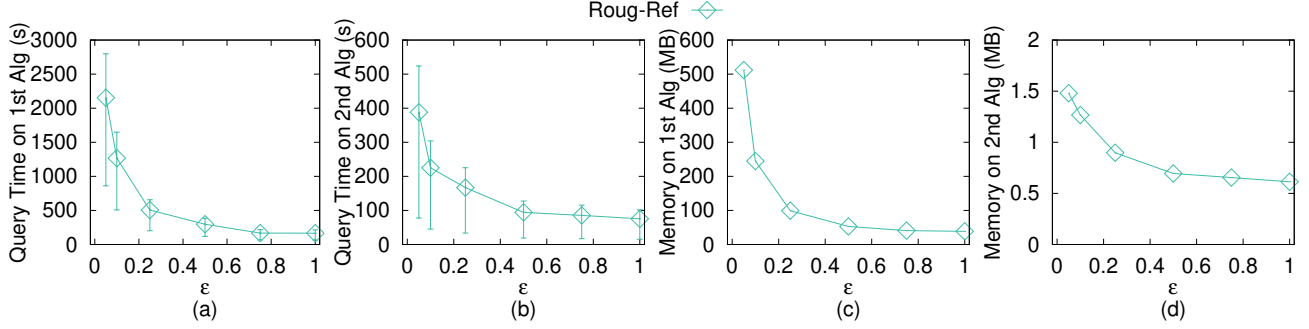


Fig. 20. Baseline comparisons (effect of  $\epsilon$  on *BH* dataset with separated query time and memory usage in two steps)

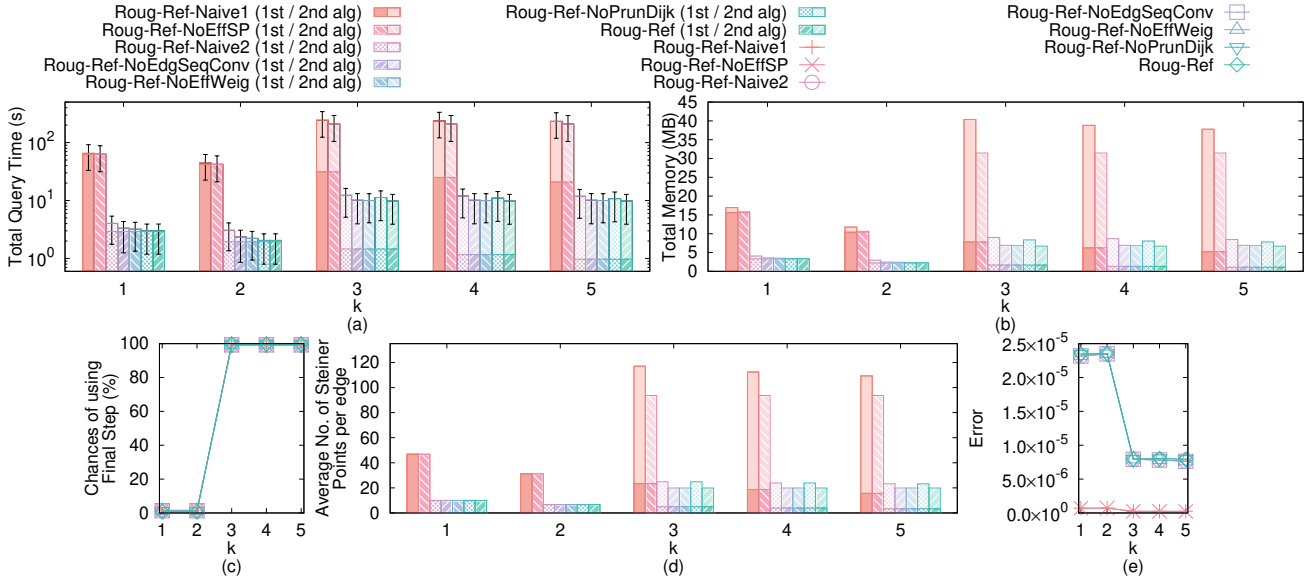


Fig. 21. Ablation study (effect of  $k$  on *EP-small* dataset)

and 0.2s, respectively.

Figure 42 and Figure 43 show the result for seabed motivation study when varying  $\epsilon$ . *Roug-Ref* still has the smallest query time and memory usage.

### B. Generating Datasets with Different Dataset Sizes

The procedure for generating the datasets with different dataset sizes is as follows. We mainly follow the procedure for generating datasets with different dataset sizes in the study [22], [30], [31]. Let  $T_t = (V_t, E_t, F_t)$  be our target terrain that we want to generate with  $ex_t$  edges along  $x$ -coordinate,  $ey_t$  edges along  $y$ -coordinate and dataset size of

$DS_t$ , where  $DS_t = 2 \cdot ex_t \cdot ey_t$ . Let  $T_o = (V_o, E_o, F_o)$  be the original terrain that we currently have with  $ex_o$  edges along  $x$ -coordinate,  $ey_o$  edges along  $y$ -coordinate and dataset size of  $DS_o$ , where  $DS_o = 2 \cdot ex_o \cdot ey_o$ . We then generate  $(ex_t + 1) \cdot (ey_t + 1)$  2D points  $(x, y)$  based on a Normal distribution  $N(\mu_N, \sigma_N^2)$ , where  $\mu_N = (\bar{x} = \frac{\sum_{v_o \in V_o} x_{v_o}}{(ex_o+1) \cdot (ey_o+1)}, \bar{y} = \frac{\sum_{v_o \in V_o} y_{v_o}}{(ex_o+1) \cdot (ey_o+1)})$  and  $\sigma_N^2 = (\frac{\sum_{v_o \in V_o} (x_{v_o} - \bar{x})^2}{(ex_o+1) \cdot (ey_o+1)}, \frac{\sum_{v_o \in V_o} (y_{v_o} - \bar{y})^2}{(ex_o+1) \cdot (ey_o+1)})$ . In the end, we project each generated point  $(x, y)$  to the surface of  $T_o$  and take the projected point (also add edges between neighbours of two

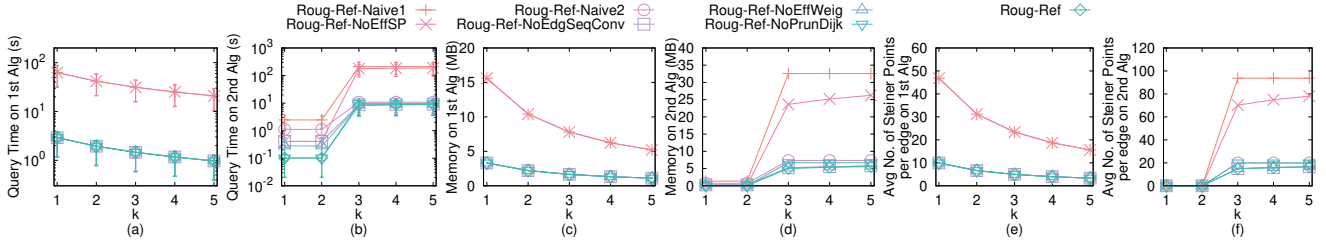


Fig. 22. Ablation study (effect of  $k$  on  $EP$ -small dataset with separated query time, memory usage, and the average number of Steiner points per edge in two steps)

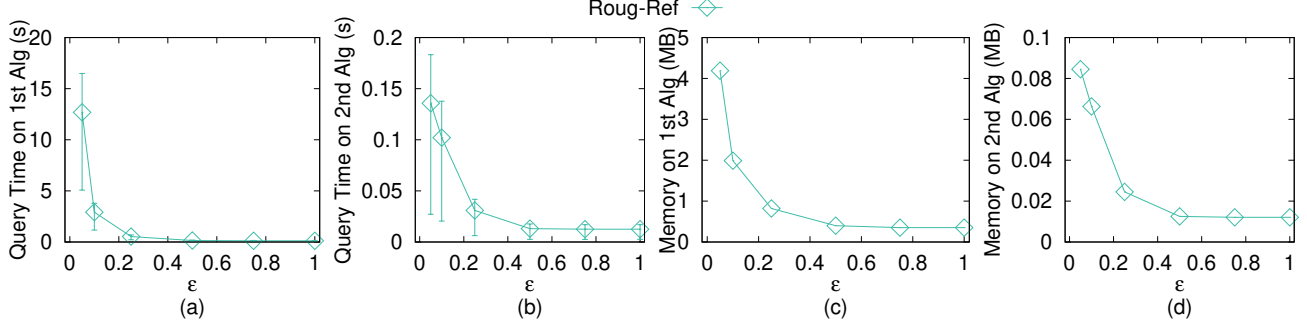


Fig. 23. Baseline comparisons (effect of  $\epsilon$  on  $EP$ -small dataset with separated query time and memory usage in two steps)

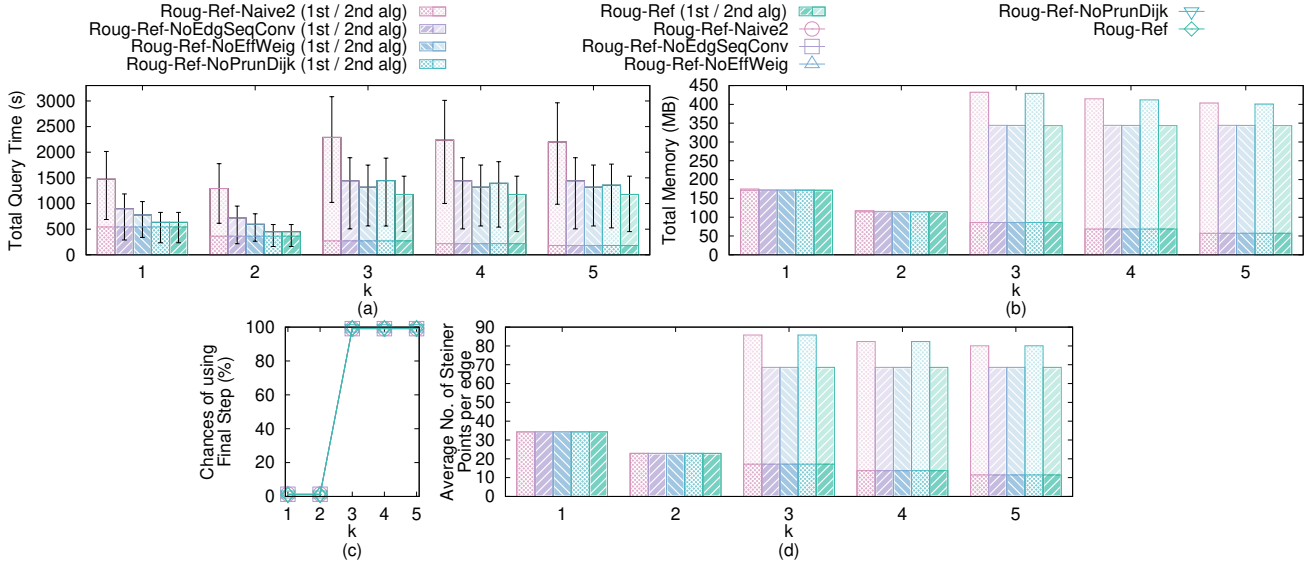


Fig. 24. Ablation study (effect of  $k$  on  $EP$  dataset)

points to form edges and faces) as the newly generate  $T_t$ .

## APPENDIX E COMPARISON OF ALL ALGORITHMS

Table IV shows a comparison of all algorithms.

## APPENDIX F PROOFS

**Lemma 1.** *There are at most  $k_{SP} \leq 2(1 + \log_\lambda \frac{L}{2 \cdot r})$  Steiner points on each edge in  $E$  when placing Steiner point based on  $\epsilon$  in algorithm Roug, where  $r$  is the minimum  $r_v$  for all  $v \in V$ .*

*Proof.* We prove it for the extreme case, i.e.,  $k_{SP}$  is maximized. This case happens when the edge has maximum length  $L$  and it joins two vertices has minimum radius  $r$ . Since each edge contains two endpoints, we have two sets of Steiner points from both endpoints, and we have the factor 2. When placing Steiner point based on  $\epsilon$  in algorithm Roug, each set of Steiner points contains at most  $(1 + \log_\lambda \frac{L}{2 \cdot r})$  Steiner points, where the 1 comes from the first Steiner point that is the nearest one from the endpoint. Therefore, we have  $k_{SP} \leq 2(1 + \log_\lambda \frac{L}{2 \cdot r})$ .  $\square$

**Lemma 2.** *When placing Steiner point based on  $\epsilon$  in algorithm Roug, based on  $1 + (2 + \frac{2W}{(1-2\epsilon') \cdot w})\epsilon' = 1 + \epsilon$ ,*



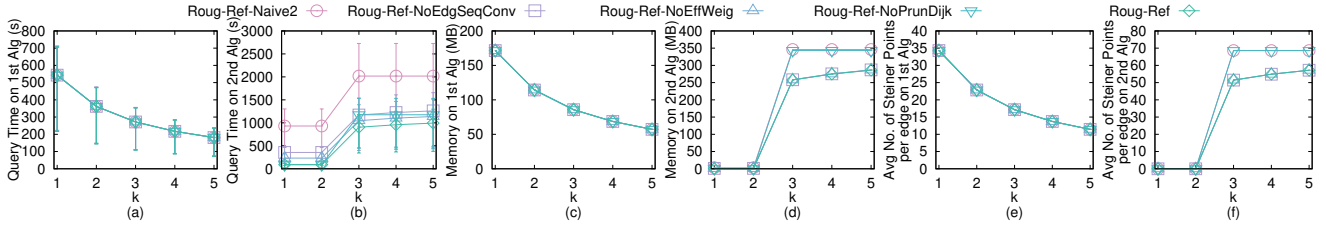


Fig. 25. Ablation study (effect of  $k$  on  $EP$  dataset with separated query time, memory usage, and the average number of Steiner points per edge in two steps)

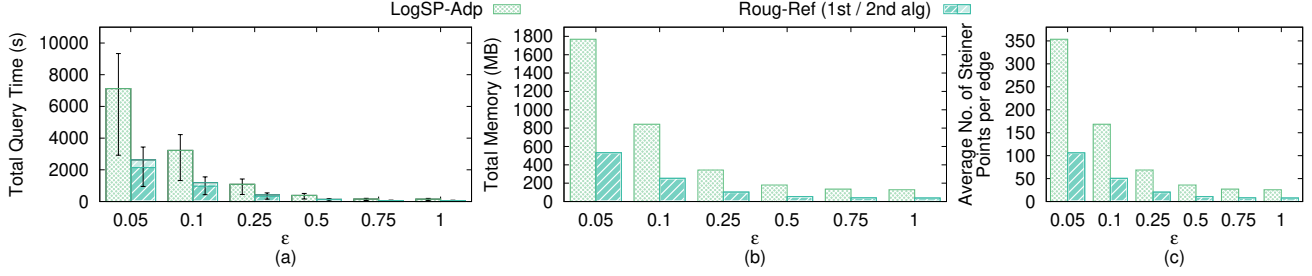


Fig. 26. Baseline comparisons (effect of  $\epsilon$  on  $EP$  dataset)

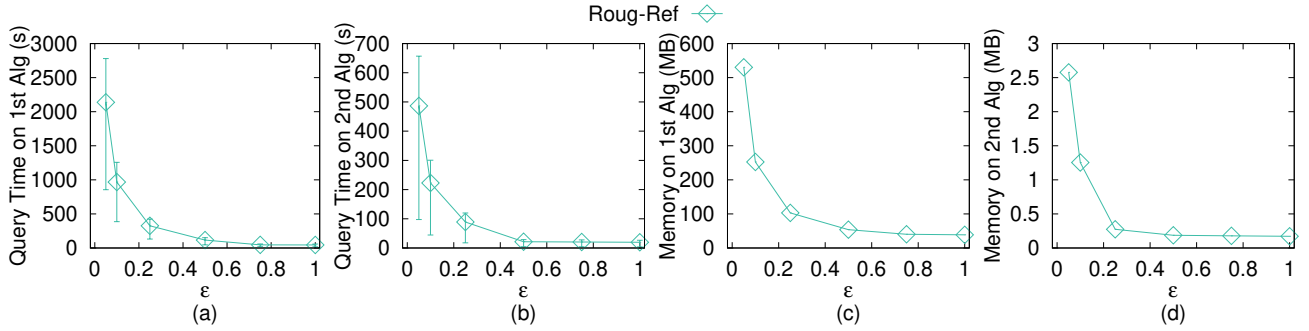


Fig. 27. Baseline comparisons (effect of  $\epsilon$  on  $EP$  dataset with separated query time and memory usage in two steps)

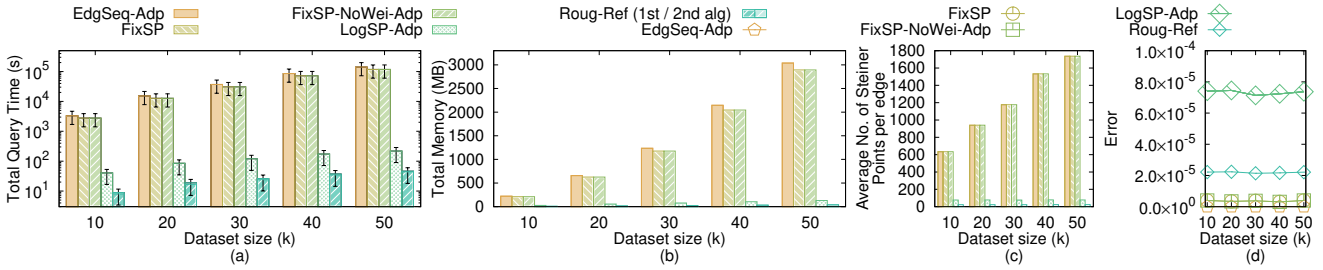


Fig. 28. Baseline comparisons (effect of dataset size on multi-resolution of  $BH$ -small datasets)

we obtain  $\epsilon' = \frac{1+\epsilon+\frac{W}{w}-\sqrt{(1+\epsilon+\frac{W}{w})^2-4\epsilon}}{4}$  with  $0 < \epsilon' < \frac{1}{2}$  and  $\epsilon > 0$ .

*Proof.* The mathematical derivation is like we regard  $\epsilon'$  as an unknown and solve a quadratic equation. The derivation is as follows.

$$\begin{aligned}
 1 + \left(2 + \frac{2W}{(1-2\epsilon') \cdot w}\right)\epsilon' &= 1 + \epsilon \\
 \left(2 + \frac{2W}{(1-2\epsilon') \cdot w}\right)\epsilon' &= \epsilon \\
 2 + \frac{2W}{(1-2\epsilon') \cdot w} &= \frac{\epsilon}{\epsilon'}
 \end{aligned}$$

$$\begin{aligned}
 \frac{2W}{(1-2\epsilon') \cdot w} &= \frac{\epsilon - 2\epsilon'}{\epsilon'} \\
 2\frac{W}{w}\epsilon' &= \epsilon - (2+2\epsilon)\epsilon' + 4\epsilon'^2 \\
 4\epsilon'^2 - (2+2\epsilon+2\frac{W}{w})\epsilon' + \epsilon &= 0 \\
 \epsilon' &= \frac{2+2\epsilon+2\frac{W}{w} \pm \sqrt{4(1+\epsilon+\frac{W}{w})^2-16\epsilon}}{8} \\
 \epsilon' &= \frac{1+\epsilon+\frac{W}{w} \pm \sqrt{(1+\epsilon+\frac{W}{w})^2-4\epsilon}}{4}
 \end{aligned}$$

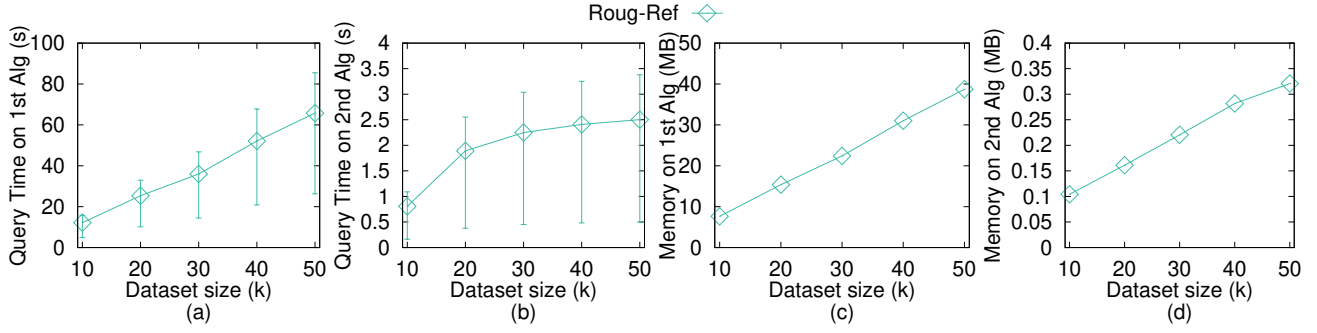


Fig. 29. Baseline comparisons (effect of dataset size on multi-resolution of *BH-small* datasets with separated query time and memory usage in two steps)

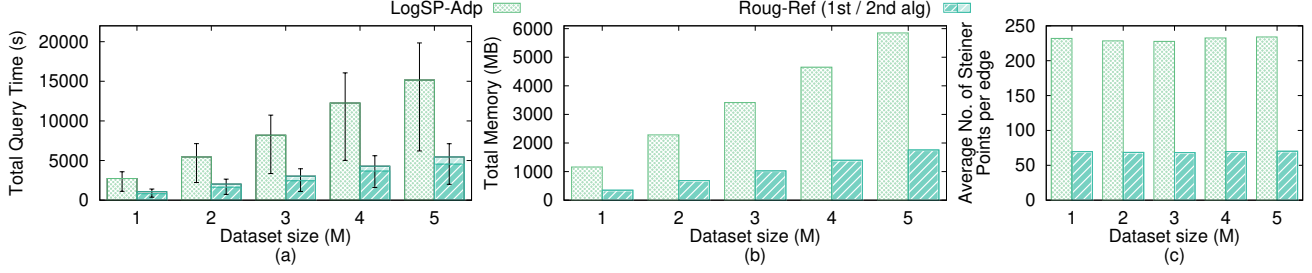


Fig. 30. Scalability test (effect of dataset size on multi-resolution of *BH* datasets)

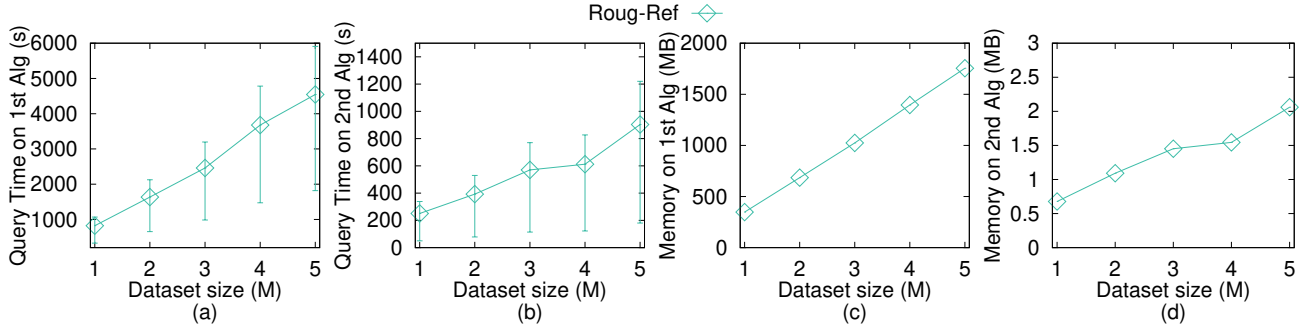


Fig. 31. Scalability test (effect of dataset size on multi-resolution of *BH* datasets with separated query time and memory usage in two steps)

Finally, we take  $\epsilon' = \frac{1+\epsilon+\frac{W}{w}-\sqrt{(1+\epsilon+\frac{W}{w})^2-4\epsilon}}{4}$  since  $0 < \epsilon' < \frac{1}{2}$  (we can plot the figure for this expression, and will found that the upper limit is always  $\frac{1}{2}$  if we use  $-$ ).  $\square$

**Lemma 3.** Let  $h$  be the minimum height of any face in  $F$  whose vertices have non-negative integer coordinates no greater than  $N$ . Then,  $h \geq \frac{1}{N\sqrt{3}}$ .

*Proof.* Let  $a$  and  $b$  be two non-zero vectors with non-negative integer coordinates no greater than  $N$ , and  $a$  and  $b$  are not co-linear. Since we know  $\frac{|a \times b|}{2}$  is the face area of  $a$  and  $b$ , we have  $h = \min_{a,b} \frac{|a \times b|}{|b|} = \min_{a,b} \frac{\sqrt{\omega}}{\sqrt{x_a^2 + y_a^2 + z_a^2}} \geq \frac{1}{N\sqrt{3}} \min_{a,b} \sqrt{\omega} \geq \frac{1}{N\sqrt{3}}$ , where  $\omega = (y_a z_b - z_a y_b)^2 + (z_a x_b - x_a z_b)^2 + (x_a y_b - y_a x_b)^2$ .  $\square$

**Theorem 2.** The running time for algorithm *Roug* is  $O(n \log n)$  and the memory usage is  $O(n)$ .

*Proof.* Originally, if we do not remove Steiner points in algorithm *Roug*, i.e., we place Steiner point based on  $\epsilon$ , then

following Lemma 1, the number of Steiner points  $k_{SP}$  on each edge is  $O(\log_{\lambda} \frac{L}{r})$ , where  $\lambda = (1 + \frac{1+\epsilon+\frac{W}{w}-\sqrt{(1+\epsilon+\frac{W}{w})^2-4\epsilon}}{4} \sin \theta)$ ,  $r = \frac{1+\epsilon+\frac{W}{w}-\sqrt{(1+\epsilon+\frac{W}{w})^2-4\epsilon}}{4} \cdot h$  and  $\theta$  is the minimum  $\theta_v$  for all  $v \in V$ . Following Lemma 2 and Lemma 3,  $r = O(\frac{\epsilon}{N})$ , and thus  $k_{SP} = O(\log \frac{LN}{\epsilon})$ . But, since we have removed Steiner points for  $\eta$  calculation and rough path calculation, the remaining Steiner points on each edge is  $O(1)$ . So  $|G_{Roug} \cdot V| = n$ . Since we know for a graph with  $n$  vertices, the running time and memory usage of Dijkstra's algorithm on this graph are  $O(n \log n)$  and  $n$ , so the running time of algorithm *Roug* is  $O(n \log n)$  and the memory usage is  $O(n)$ .  $\square$

**Theorem 3.** The running time for the full edge sequence conversion step in algorithm *Ref* is  $O(n \log n)$  and the memory usage is  $O(n)$ .

*Proof.* Firstly, we prove the running time. Given  $\Pi_{Roug}(s, t)$ , there are three cases on how to apply the full edge sequence

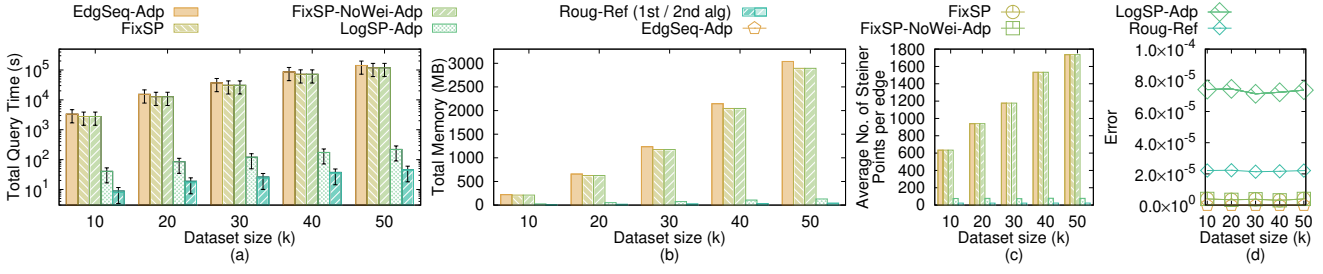


Fig. 32. Baseline comparisons (effect of dataset size on multi-resolution of  $EP$ -small datasets)

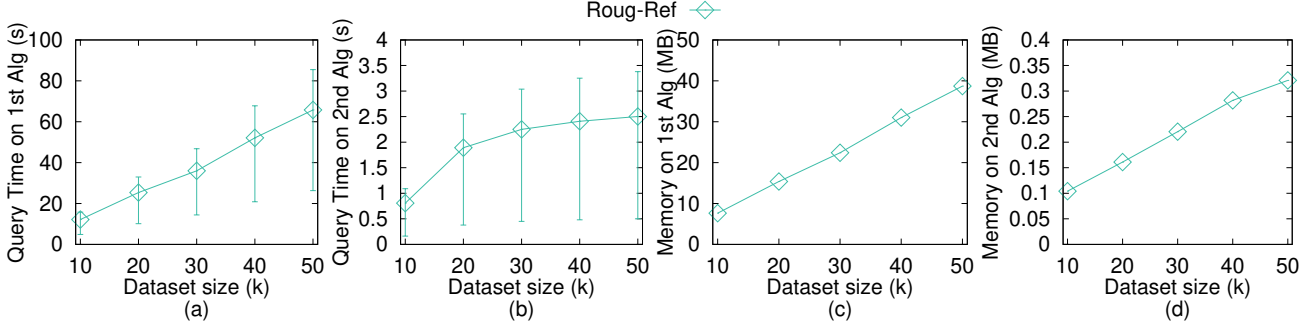


Fig. 33. Baseline comparisons (effect of dataset size on multi-resolution of  $EP$ -small datasets with separated query time and memory usage in two steps)

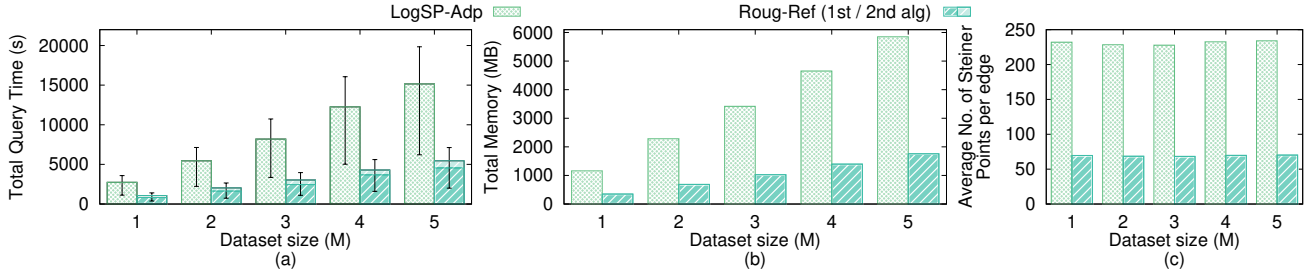


Fig. 34. Scalability test (effect of dataset size on multi-resolution of  $EP$  datasets)

conversion step in algorithm *Ref* on  $\Pi_{Roug}(s, t)$ , i.e., (1) some segments of  $\Pi_{Roug}(s, t)$  passes on the edges (i.e., no need to use algorithm *Ref* full edge sequence conversion step), (2) some segments of  $\Pi_{Roug}(s, t)$  belongs to single endpoint case, and (3) some segments of  $\Pi_{Roug}(s, t)$  belongs to successive endpoint case. For the first case, there is no need to case about it. For the second case, we just need to add more Steiner points on the edges adjacent to the vertices passed by  $\Pi_{Roug}(s, t)$ , and using Dijkstra's algorithm to refine it, and the running time is the same as the one in algorithm *Roug*, which is  $O(n \log n)$ . For the third case, we just need to add more Steiner points on the edge adjacent to the vertex passed by  $\Pi_{Roug}(s, t)$ , and find a shorter path by running for  $\zeta$  times, and there are at most  $O(n)$  such vertices, so the running time is  $O(\zeta n) = O(n)$ . Therefore, the running time for the full edge sequence conversion step in algorithm *Ref* is  $O(n \log n)$ .

Secondly, we prove the *memory usage*. Algorithm *Roug* needs  $O(n)$  memory since it is a common Dijkstra's algorithm, whose memory usage is  $O(|G_{Roug}.V|)$ , where  $|G_{Roug}.V|$  is size of vertices in the Dijkstra's algorithm. Handling one single endpoint case needs  $O(1)$  memory. Since there can be at most

$n$  single endpoint cases, the memory usage is  $O(n)$ . Handling successive endpoint cases needs  $O(n)$  memory since algorithm *Roug* needs  $O(n)$  memory. Therefore, the memory usage for the full edge sequence conversion step in algorithm *Ref* is  $O(n)$ .  $\square$

**Theorem 4.** *The running time for the Snell's law path refinement step in algorithm Ref is  $O(l)$ , and the memory usage is  $O(l)$ .*

*Proof.* Firstly, we prove the *running time*. Let  $l$  be the number of edges in  $S$ . Since the effective weight pruning sub-step can directly find the optimal position of the intersection point on each edge in  $S$  in  $O(1)$  time, the running time of the Snell's law path refinement step in algorithm *Ref* is  $O(l)$ .

Secondly, we prove the *memory usage*, since the refined path will pass  $l$  edges, so the memory usage of the Snell's law path refinement step in algorithm *Ref* is  $O(l)$ .  $\square$

*Proof of Theorem 1.* Firstly, we prove the *total running time*. (1) In most of the cases, there is no need to use the error guaranteed path refinement step in algorithm *Ref*. In this case,

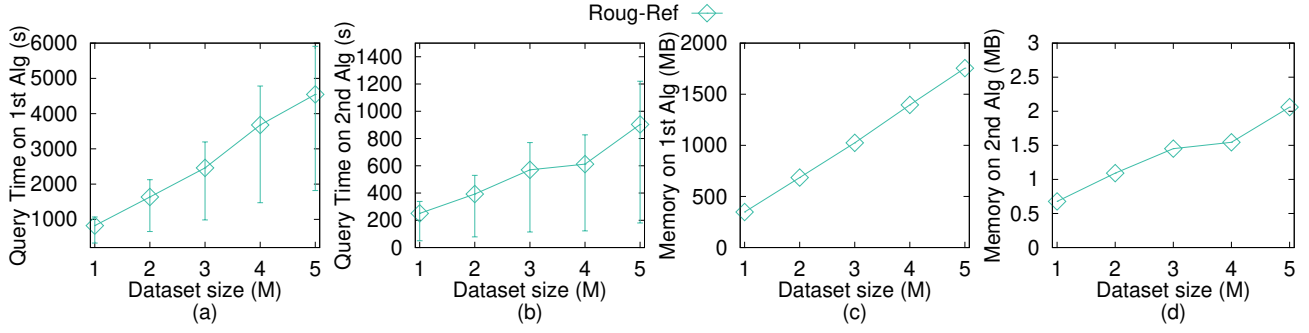


Fig. 35. Scalability test (effect of dataset size on multi-resolution of *EP* datasets with separated query time and memory usage in two steps)

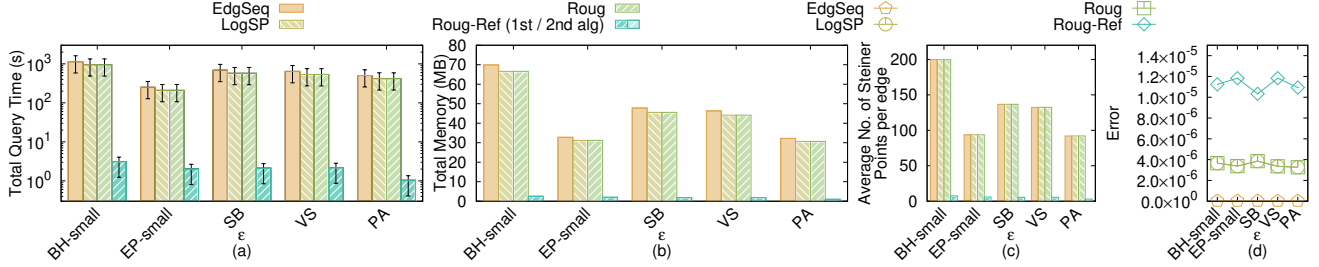


Fig. 36. Large distance error algorithm comparisons

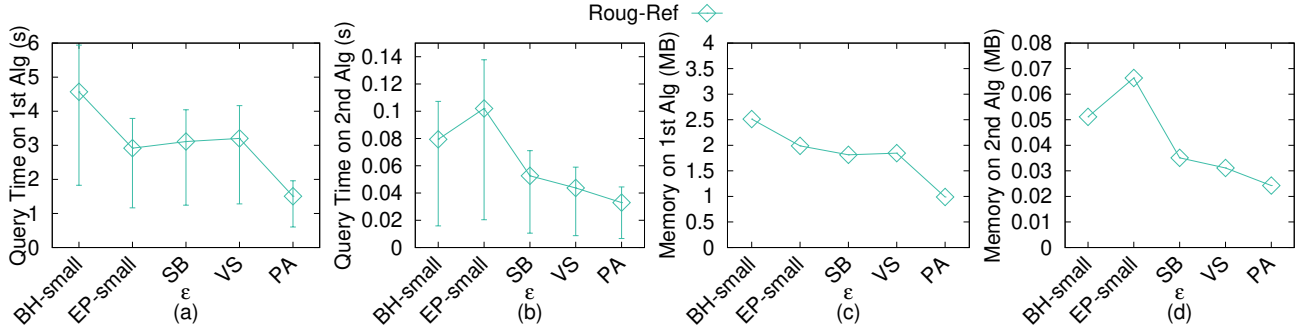


Fig. 37. Large distance error algorithm comparisons with separated query time and memory usage in two steps

the total running time is the sum of the running time using algorithm *Roug* and the first three steps in algorithm *Ref*. From Theorem 2, Theorem 3 and Theorem 4, we obtain the total running time  $O(n \log n + l)$ . (2) In some special cases, we need to use the error guaranteed path refinement step in algorithm *Ref* for error guarantee. The sum of the running time of algorithm *Roug* and the error guaranteed path refinement step in algorithm *Ref* is exactly the same as the running time that we perform Dijkstra's algorithm on the weighted graph  $G_{Ref}$  constructed by the original Steiner points (i.e.,  $k_{SP} = O(\log \frac{LN}{\epsilon})$  Steiner points per edge) and  $V$ , which is  $O(n \log \frac{LN}{\epsilon} \log(n \log \frac{LN}{\epsilon}) + l)$ . But the constant term  $O(\log \frac{LN}{\epsilon})$  is not important and can be omitted, so we obtain the total running time  $O(n \log n + l)$ . (3) In general, the total running time is  $O(n \log n + l)$ .

Secondly, we prove the *total memory usage*. (1) In most of the cases, there is no need to use the error guaranteed path refinement step in algorithm *Ref*. In this case, the total memory usage is the sum of the memory usage using algorithm

*Roug* and the first three steps in algorithm *Ref*. From Theorem 2, Theorem 3 and Theorem 4, we obtain the average case total memory usage  $O(n + l)$ . (2) In some cases, we need to use the error guaranteed path refinement step in algorithm *Ref* for error guarantee. The sum of the memory usage of algorithm *Roug* and the error guaranteed path refinement step in algorithm *Ref* is exactly the same as the memory usage that we perform Dijkstra's algorithm on the weighted graph  $G_{Ref}$  constructed by the original Steiner points (i.e.,  $k_{SP} = O(\log \frac{LN}{\epsilon})$  Steiner points per edge) and  $V$ , which is  $O(n \log \frac{LN}{\epsilon} + l)$ . But the constant term  $O(\log \frac{LN}{\epsilon})$  is not important and can be omitted, so we obtain the total memory usage  $O(n + l)$ . (3) In general, the total memory usage is  $O(n + l)$ .

Finally, we prove the *error bound*. Recall one baseline algorithm *LogSP*. We define the path calculated by algorithm *LogSP* between  $s$  and  $t$  to be  $\Pi_{LogSP}(s, t)$ . The study [4], [17] show that  $|\Pi_{LogSP}(s, t)| \leq (1 + (2 + \frac{2W}{(1-2\epsilon') \cdot w})\epsilon')|\Pi^*(s, t)|$ . A proof sketch appears in Theorem 1 of study [4] and a



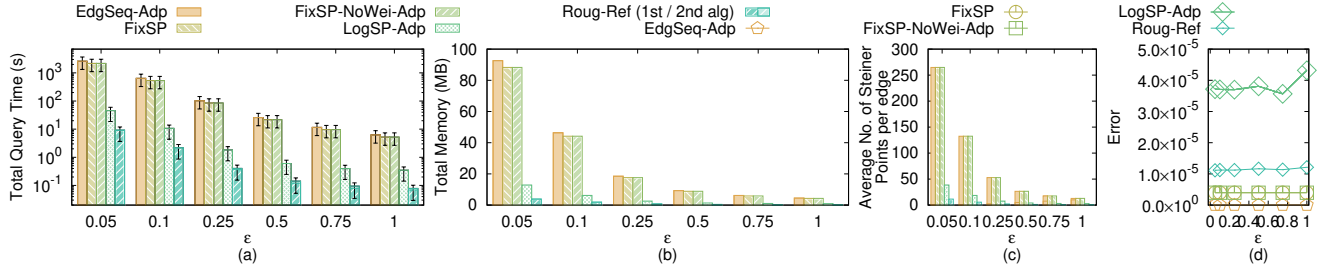


Fig. 38. Earthquake and avalanche user study (effect of  $\epsilon$  on VS dataset)

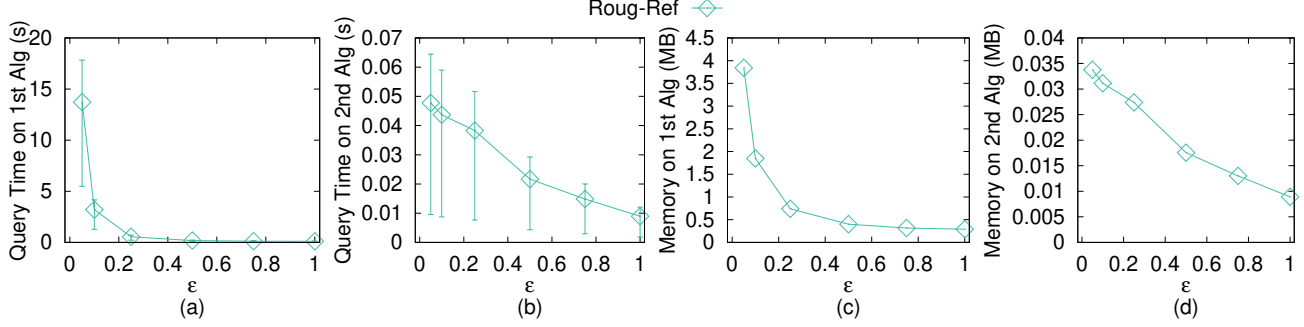


Fig. 39. Earthquake and avalanche user study (effect of  $\epsilon$  on VS dataset with separated query time and memory usage in two steps)

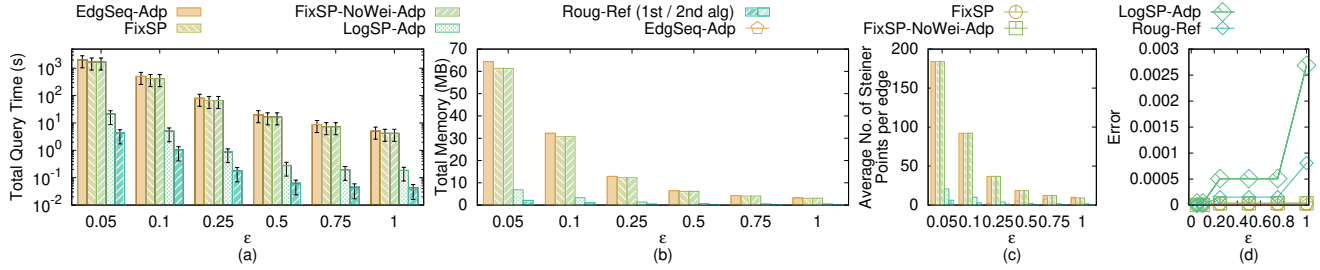


Fig. 40. Path Advisor user study (effect of  $\epsilon$  on PA dataset)

detailed proof appears in Theorem 3.1 of study [17]. We adapt algorithm *LogSP* to be algorithm *LogSP-Adp* by substituting  $(2 + \frac{2W}{(1-2\epsilon') \cdot w})\epsilon' = \epsilon$  with  $0 < \epsilon' < \frac{1}{2}$  and  $\epsilon > 0$ , we have  $|\Pi_{LogSP-Adp}(s, t)| \leq (1 + \epsilon)|\Pi^*(s, t)|$  where  $\epsilon > 0$  and  $\Pi_{LogSP-Adp}(s, t)$  is the path result returned by algorithm *LogSP-Adp*. Recall that algorithm *LogSP-Adp* corresponds to the efficient Steiner point placement scheme in algorithm *Roug*. This error bound is always true no matter whether the edge sequence passed by  $\Pi_{LogSP-Adp}(s, t)$  is the same as the edge sequence passed by  $\Pi^*(s, t)$  or not. Then, in algorithm *Roug*, we first remove some Steiner points in the rough path calculation step, and then calculate  $\eta\epsilon$  based on the remaining Steiner points, and then use  $\eta\epsilon$  as the input error to calculate  $\Pi_{Roug}(s, t)$  in the rough path calculation step, so by adapt  $\eta\epsilon$  as the input error in algorithm *LogSP-Adp*, we have  $|\Pi_{Roug}(s, t)| \leq (1 + \eta\epsilon)|\Pi^*(s, t)|$ . Next, in the path checking step of algorithm *Ref*, if  $|\Pi_{Ref-2}(s, t)| \leq \frac{(1+\epsilon)}{(1+\eta\epsilon)}|\Pi_{Roug}(s, t)|$ , we return  $\Pi_{Ref-2}(s, t)$  as output  $\Pi(s, t)$ , which implies that  $|\Pi_{Ref-2}(s, t)| = |\Pi(s, t)| \leq (1+\epsilon)|\Pi^*(s, t)|$ . Otherwise, we use the error guaranteed path refinement step in algorithm *Ref*, and we return  $\Pi_{Ref-3}(s, t)$  as output  $\Pi(s, t)$ , where the error bound

is the same as in algorithm *LogSP-Adp*, i.e.,  $|\Pi_{Ref-3}(s, t)| = |\Pi(s, t)| \leq (1 + \epsilon)|\Pi^*(s, t)|$ . Therefore, algorithm *Roug-Ref* guarantees that  $|\Pi(s, t)| \leq (1 + \epsilon)|\Pi^*(s, t)|$ .  $\square$

**Theorem 5.** *The running time for algorithm *FixSP* is  $O(n^3 \log n)$ , and the memory usage is  $O(n^3)$ . It guarantees that  $|\Pi_{FixSP}(s, t)| \leq (1 + \epsilon)|\Pi^*(s, t)|$ , where  $\Pi_{FixSP}(s, t)$  is the path result returned by algorithm *FixSP*.*

*Proof.* Firstly, we prove both the *running time* and *memory usage*. By using algorithm *FixSP*, we need to place  $O(n^2)$  Steiner points per edge on  $E$  [18]. Since there are total  $n$  edges, there are total  $O(n^3)$  Steiner points in the weighted graph, so the running time and memory usage of using Dijkstra's algorithm, i.e., algorithm *FixSP*, on this graph are  $O(n^3 \log n)$  and  $O(n^3)$ .

Secondly, we prove the *error bound*. Theorem 2.6 of study [17] shows that  $|\Pi_{FixSP}(s, t)| \leq (1 + \epsilon)|\Pi^*(s, t)|$ .  $\square$

**Theorem 6.** *The running time for algorithm *FixSP-NoWei-Adp* is  $O(n^3 \log n)$ , and the memory usage is  $O(n^3)$ . It guarantees that  $|\Pi_{FixSP-NoWei-Adp}(s, t)| \leq (1 + \epsilon)|\Pi^*(s, t)|$ , where*

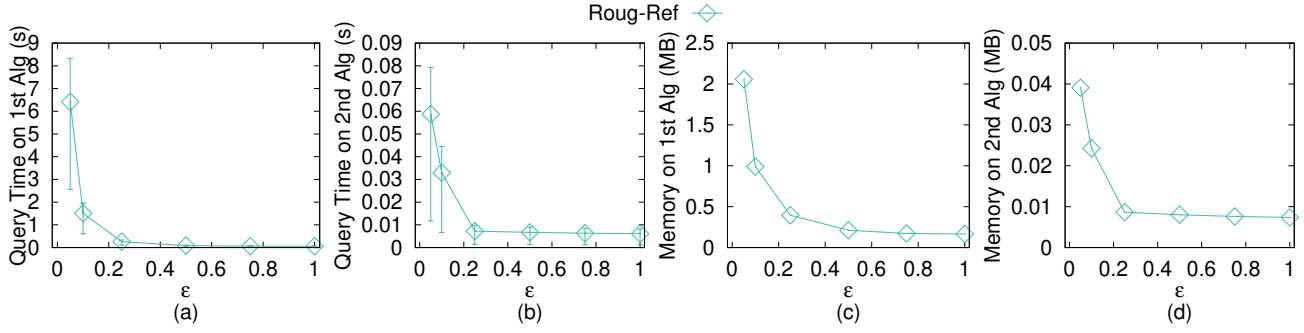


Fig. 41. Path Advisor user study (effect of  $\epsilon$  on PA dataset with separated query time and memory usage in two steps)

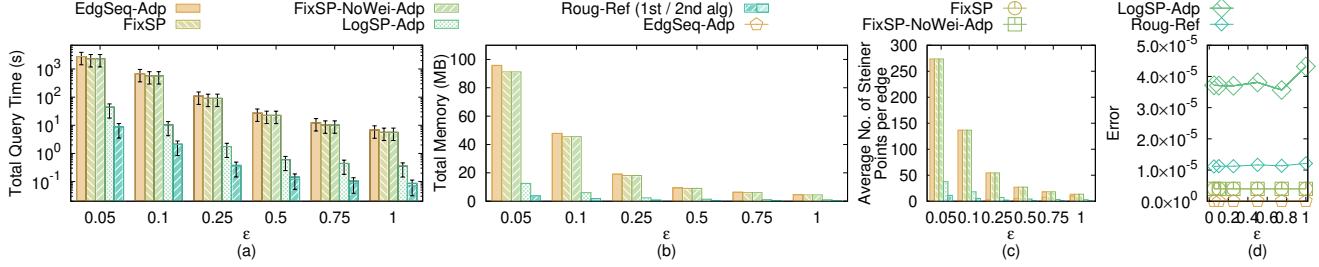


Fig. 42. Cable placement motivation study (effect of  $\epsilon$  on SB dataset)

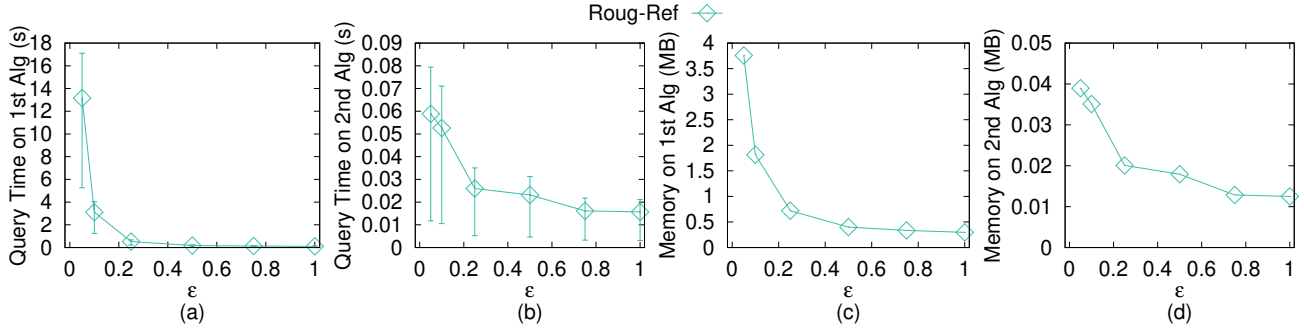


Fig. 43. Cable placement motivation study (effect of  $\epsilon$  on SB dataset with separated query time and memory usage in two steps)

$\Pi_{\text{FixSP-NoWei-Adp}}(s, t)$  is the path result returned by algorithm *FixSP-NoWei-Adp*.

*Proof.* Since algorithm *FixSP-NoWei-Adp* is equivalent to algorithm *FixSP*, its running time, memory usage and error bound is the same as that of algorithm *FixSP*.  $\square$

**Theorem 7.** The running time for algorithm *LogSP* is  $O(n \log \frac{LN}{\epsilon'} \log(n \log \frac{LN}{\epsilon'}))$ , the memory usage is  $O(n \log \frac{LN}{\epsilon'})$ . It guarantees that  $|\Pi_{\text{LogSP}}(s, t)| \leq (1 + (2 + \frac{2W}{(1-2\epsilon') \cdot w})\epsilon')|\Pi^*(s, t)|$ , where  $\Pi_{\text{LogSP}}(s, t)$  is the path result returned by algorithm *LogSP*.

*Proof.* Firstly, we prove both the running time and memory usage. By using algorithm *LogSP*, we need to place  $k_{SP} = O(\log \frac{LN}{\epsilon'})$  Steiner points per edge on  $E$ . Since there are total  $n$  edges, there are total  $O(n^3)$  Steiner points in the weighted graph, so the running time and memory usage of using Dijkstra's algorithm, i.e., algorithm *LogSP*, on this graph are  $O(n \log \frac{LN}{\epsilon'} \log(n \log \frac{LN}{\epsilon'}))$  and  $O(n \log \frac{LN}{\epsilon'})$ .

Secondly, we prove the error bound. Theorem 1 of study [4] shows that  $|\Pi_{\text{LogSP}}(s, t)| \leq (1 + (2 + \frac{2W}{(1-2\epsilon') \cdot w})\epsilon')|\Pi^*(s, t)|$ .  $\square$

**Theorem 8.** The running time for algorithm *LogSP-Adp* is  $O(n \log \frac{LN}{\epsilon} \log(n \log \frac{LN}{\epsilon}))$ , and the memory usage is  $O(n \log \frac{LN}{\epsilon})$ . It guarantees that  $|\Pi_{\text{LogSP-Adp}}(s, t)| \leq (1 + \epsilon)|\Pi^*(s, t)|$ , where  $\Pi_{\text{LogSP-Adp}}(s, t)$  is the path result returned by algorithm *LogSP-Adp*.

*Proof.* Firstly, we prove both the running time and memory usage. By using algorithm *LogSP-Adp*, we need to place  $k_{SP} = O(\log \frac{LN}{\epsilon})$  Steiner points per edge on  $E$ . Since there are total  $n$  edges, there are total  $O(n^3)$  Steiner points in the weighted graph, so the running time and memory usage of using Dijkstra's algorithm, i.e., algorithm *LogSP-Adp*, on this graph are  $O(n \log \frac{LN}{\epsilon} \log(n \log \frac{LN}{\epsilon}))$  and  $O(n \log \frac{LN}{\epsilon})$ .

Secondly, we prove the error bound. Theorem 1 of study [4] shows that  $|\Pi_{\text{LogSP}}(s, t)| \leq (1 + (2 + \frac{2W}{(1-2\epsilon') \cdot w})\epsilon')|\Pi^*(s, t)|$ . After substituting  $(2 + \frac{2W}{(1-2\epsilon') \cdot w})\epsilon' = \epsilon$  with  $0 < \epsilon' < \frac{1}{2}$  and

TABLE IV  
COMPARISON OF ALL ALGORITHMS

| Algorithm                     | Time  |              | Size                                 |              | Error   |
|-------------------------------|---|--------------|--------------------------------------|--------------|---|
| <i>EdgSeq</i> [29]            | $O(n^4 \log(\frac{n^2 NWL}{w\epsilon}))$  | Large        | $O(n^2)$                             | Large        | No error bound  |
| <i>EdgSeq-Adp</i> [29]        | $O(n^3 \log n + n^4 \log(\frac{n^2 NWL}{w\epsilon}))$   | Large        | $O(n^3)$                             | Large        | $1 + \epsilon$  |
| <i>FixSP</i> [13], [18]       | $O(n^3 \log n)$   | Large        | $O(n^3)$                             | Large        | $1 + \epsilon$  |
| <i>FixSP-NoWei-Adp</i> [14]   | $O(n^3 \log n)$   | Large        | $O(n^3)$                             | Large        | $1 + \epsilon$  |
| <i>LogSP</i> [4]              | $O(n \log \frac{LN}{\epsilon'} \log(n \log \frac{LN}{\epsilon'}))$                                      | Medium       | $O(n \log \frac{LN}{\epsilon'})$     | Medium       | $1 + (2 + \frac{2W}{(1-2\epsilon) \cdot w})\epsilon'$ |
| <i>LogSP-Adp</i> [4]          | $O(n \log \frac{LN}{\epsilon} \log(n \log \frac{LN}{\epsilon}))$  | Medium       | $O(n \log \frac{LN}{\epsilon})$      | Medium       | $1 + \epsilon$  |
| <i>Roug-Ref-Naive1</i>        | $O(n^3 \log n + nl^2 \log(\frac{n^2 NWL}{w\epsilon}))$  | Large        | $O(n^3 + nl)$                        | Large        | $1 + \epsilon$  |
| <i>Roug-Ref-NoEffSP</i>       | $O(n^2 \log n + l)$   | Large        | $O(n^2 + l)$                         | Large        | $1 + \epsilon$  |
| <i>Roug-Ref-Naive2</i>        | $O(n \log \frac{LN}{\epsilon} \log(n \log \frac{LN}{\epsilon}) + nl^2 \log(\frac{n^2 NWL}{w\epsilon}))$ | Large        | $O(n \log \frac{LN}{\epsilon} + nl)$ | Medium       | $1 + \epsilon$  |
| <i>Roug-Ref-NoEdgSeqConv</i>  | $O(n \log n + nl)$  | Medium       | $O(nl)$                              | Small        | $1 + \epsilon$  |
| <i>Roug-Ref-NoEffWeig</i>     | $O(n \log n + l^2 \log(\frac{n^2 NWL}{w\epsilon}))$   | Medium       | $O(n + l)$                           | Small        | $1 + \epsilon$  |
| <i>Roug-Ref-NoPrunDijk</i>    | $O(n \log \frac{LN}{\epsilon} \log(n \log \frac{LN}{\epsilon}) + l)$                                    | Medium       | $O(n \log \frac{LN}{\epsilon} + l)$  | Medium       | $1 + \epsilon$  |
| <i>Roug</i>                   | $O(n \log n)$   | Small        | $O(n)$                               | Small        | $1 + \eta\epsilon$                                    |
| <b><i>Roug-Ref</i> (ours)</b> | <b><math>O(n \log n + l)</math></b>   | <b>Small</b> | <b><math>O(n + l)</math></b>         | <b>Small</b> | <b><math>1 + \epsilon</math></b>                      |

$\epsilon > 0$ , we have  $|\Pi_{LogSP-Adp}(s, t)| \leq (1 + \epsilon)|\Pi^*(s, t)|$  where  $\epsilon > 0$ .  $\square$

**Theorem 9.** *The running time for algorithm EdgSeq is  $O(n^4 \log(\frac{n^2 NWL}{w\epsilon}))$ , and the memory usage is  $O(n^2)$ . It does not have error bound guarantee.*

*Proof.* Firstly, we prove both the *running time*. Algorithm *EdgSeq-Adp* first uses a similar method in algorithm *FixSP* (but only places a constant number of Steiner points per edge) to calculate an edge sequence in  $O(1)$  time, then uses Snell's law in a binary search manner to calculate the result path in  $O(l'^2 \log \frac{l'}{\delta})$  time according to Lemma 2.4 of study [29], where  $l'$  is the number of edges in the edge sequence calculated by algorithm *FixSP* and  $\delta = \frac{h\epsilon w}{6l'W}$ . According to Lemma 7.1 of study [24],  $l' = O(n^2)$ . Thus, the running time of algorithm *EdgSeq-Adp* is  $O(n^4 \log(\frac{n^2 NWL}{w\epsilon}))$ .

Secondly, we prove the *total memory usage*. Algorithm *EdgSeq-Adp* first uses a similar method in algorithm *FixSP* (but only places a constant number of Steiner points per edge) to calculate an edge sequence with  $O(1)$  memory usage, then uses Snell's law in a binary search manner to calculate the result path with  $O(l')$  memory usage since the result path will pass  $l'$  edges. Since  $l' = O(n^2)$ , the memory usage of algorithm *EdgSeq-Adp* is  $O(n^2)$ .  $\square$

**Theorem 10.** *The running time for algorithm EdgSeq-Adp is  $O(n^3 \log n + n^4 \log(\frac{n^2 NWL}{w\epsilon}))$ , and the memory usage is  $O(n^3)$ . It guarantees that  $|\Pi_{EdgSeq-Adp}(s, t)| \leq (1 + \epsilon)|\Pi^*(s, t)|$ , where  $\Pi_{EdgSeq-Adp}(s, t)$  is the path result returned by algorithm EdgSeq-Adp.*

*Proof.* Firstly, we prove both the *running time*. Algorithm *EdgSeq-Adp* first uses algorithm *FixSP* to calculate an edge sequence in  $O(n^3 \log n)$  time, then uses Snell's law in a binary search manner to calculate the result path in  $O(l'^2 \log \frac{l'}{\delta})$  time according to Lemma 2.4 of study [29], where  $l'$  is the number of edges in the edge sequence calculated by algorithm *FixSP* and  $\delta = \frac{h\epsilon w}{6l'W}$ . According to Lemma 7.1 of study [24],

$l' = O(n^2)$ . Thus, the running time of algorithm *EdgSeq-Adp* is  $O(n^3 \log n + n^4 \log(\frac{n^2 NWL}{w\epsilon}))$ .

Secondly, we prove the *total memory usage*. Algorithm *EdgSeq-Adp* first uses algorithm *FixSP* to calculate an edge sequence with  $O(n^3)$  memory usage, then uses Snell's law in a binary search manner to calculate the result path with  $O(l')$  memory usage since the result path will pass  $l'$  edges. Since  $l' = O(n^2)$ , the memory usage of algorithm *EdgSeq-Adp* is  $O(n^3)$ .

Thirdly, we prove the *error bound*. Algorithm *EdgSeq-Adp* first uses algorithm *FixSP* to calculate a  $(1 + \epsilon)$ -approximate weighted shortest path, then uses Snell's law to calculate the result path with a smaller error. Due to the error bound of algorithm *FixSP*, we have  $|\Pi_{EdgSeq-Adp}(s, t)| \leq (1 + \epsilon)|\Pi^*(s, t)|$ .  $\square$

**Theorem 11.** *The total running time for algorithm Roug-Ref-NoEffSP is  $O(n^2 \log n + l)$ , and the total memory usage is  $O(n^2 + l)$ . It guarantees that  $|\Pi_{Roug-Ref-NoEffSP}(s, t)| \leq (1 + \epsilon)|\Pi^*(s, t)|$ , where  $\Pi_{Roug-Ref-NoEffSP}(s, t)$  is the path result returned by algorithm Roug-Ref-NoEffSP.*

*Proof.* The difference between *Roug-Ref-NoEffSP* and *Roug-Ref* is that in the former one, we use *FixSP* to substitute *LogSP* as Steiner points placement scheme in algorithm *Roug* and the error guaranteed path refinement in *Ref*.

Firstly, we prove both the *running time* and *memory usage*. From Theorem 5, we know that by using *FixSP*, we need to place  $O(n^2)$  Steiner points per edge on  $E$  [18]. Since there are total  $n$  edges, there are total  $O(n^3)$  Steiner points in the weighted graph, so the running time and memory usage of using Dijkstra's algorithm on this graph are  $O(n^3 \log n)$  and  $O(n^3)$ . By using the framework of *Roug-Ref*, we obtain the total running time and total memory usage, i.e.,  $O(n^2 \log n + l)$  and  $O(n^2 + l)$ .

Secondly, we prove the *error bound*. From Theorem 5, we know that  $|\Pi_{FixSP}(s, t)| \leq (1 + \epsilon)|\Pi^*(s, t)|$ , where  $\Pi_{FixSP}(s, t)$  is the path result returned by algorithm *FixSP*. Since from Theorem 1, we also have  $|\Pi_{LogSP}(s, t)| \leq (1 + \epsilon)|\Pi^*(s, t)|$ , where  $\Pi_{LogSP}(s, t)$  is the path result returned by algorithm

*LogSP*, so by using the framework of *Roug-Ref*, we obtain the error bound of algorithm *Roug-Ref-NoEffSP*.  $\square$

**Theorem 12.** *The total running time for algorithm *Roug-Ref-NoEdgSeqConv* is  $O(n \log n + nl)$ , and the total memory usage is  $O(nl)$ . It guarantees that  $|\Pi_{\text{Roug-Ref-NoEdgSeqConv}}(s, t)| \leq (1 + \epsilon)|\Pi^*(s, t)|$ , where  $\Pi_{\text{Roug-Ref-NoEdgSeqConv}}(s, t)$  is the path result returned by algorithm *Roug-Ref-NoEdgSeqConv*.*

*Proof.* The difference between *Roug-Ref-NoEdgSeqConv* and *Roug-Ref* is that in the former one, we remove the full edge sequence conversion step in algorithm *Ref* (such that the input edge sequence of the Snell's law path refinement step in algorithm *Ref* may be a non-full edge sequence, then we need to try Snell's law on different combinations of edges and select the result path with the minimum distance). This will only affect the total running time and the total memory usage. Thus, we only prove the total running time and the total memory usage.

For both the *total running time* and the *total memory usage*, there are total  $n$  different cases of the edge sequence that we need to perform Snell's law on, that is, we need to use the Snell's law path refinement step in algorithm *Ref* for  $n$  times, and select the path with the shortest distance. Therefore, the total running time and the total memory usage need to include the Snell's law path refinement step in algorithm *Ref* for  $n$  times. By using the framework of *Roug-Ref*, we obtain the total running time and total memory usage, i.e.,  $O(n \log n + nl)$  and  $O(nl)$ .  $\square$

**Theorem 13.** *The total running time for algorithm *Roug-Ref-NoEffWeig* is  $O(n \log n + l^2 \log(\frac{LNWL}{w\epsilon}))$ , and the total memory usage is  $O(n + l)$ . It guarantees that  $|\Pi_{\text{Roug-Ref-NoEffWeig}}(s, t)| \leq (1 + \epsilon)|\Pi^*(s, t)|$ , where  $\Pi_{\text{Roug-Ref-NoEffWeig}}(s, t)$  is the path result returned by algorithm *Roug-Ref-NoEffWeig*.*

*Proof.* The difference between *Roug-Ref-NoEffWeig* and *Roug-Ref* is that in the former one, we remove the effective weight pruning out sub-step in the Snell's law path refinement step of algorithm *Ref*. This will only affect the total running time and the total memory usage. Thus, we only prove the total running time and the total memory usage.

Firstly, we prove the *total running time*. Let  $l$  be the number of edges in  $S$ . In the binary search initial path and binary search refined path finding sub-step, it first takes  $O(l)$  time to compute the 3D surface Snell's ray  $\Pi_m$  since there are  $l$  edges in  $S$  and we need to use Snell's law  $l$  times to calculate the intersection point on each edge. Then, it takes  $O(\log \frac{L_i}{\delta})$  time to decide the position of  $m_i$  because we stop the iteration when  $|a_i b_i| < \delta$ , and they are binary search approach, where  $L_i$  is the length of  $e_i$ . Since  $\delta = \frac{h\epsilon w}{6lW}$  and  $L_i \leq L$  for  $\forall i \in \{1, \dots, l\}$ , the running time is  $O(\log \frac{LWL}{h\epsilon w})$ . Since we run the above two nested loops  $l$  times, the total running time is  $O(l^2 \log \frac{LWL}{h\epsilon w})$ . So the running time of the Snell's law path refinement step without the effective weight pruning sub-step in algorithm *Ref* is  $O(l^2 \log \frac{LWL}{h\epsilon w})$ . By using

the framework of *Roug-Ref*, we obtain the total running time is  $O(n \log n + l^2 \log(\frac{LNWL}{w\epsilon}))$ .

Secondly, we prove the *total memory usage*. Since the refined path will pass  $l$  edges, so the memory usage of the Snell's law path refinement step without the effective weight pruning sub-step in algorithm *Ref* is  $O(l)$ . By using the framework of *Roug-Ref*, we obtain the total memory usage is  $O(n + l)$ .  $\square$

**Theorem 14.** *The total running time for algorithm *Roug-Ref-NoPrunDijk* is  $O(n \log \frac{LN}{\epsilon} \log(n \log \frac{LN}{\epsilon}) + l)$ , and the total memory usage is  $O(n \log \frac{LN}{\epsilon} + l)$ . It guarantees that  $|\Pi_{\text{Roug-Ref-NoPrunDijk}}(s, t)| \leq (1 + \epsilon)|\Pi^*(s, t)|$ , where  $\Pi_{\text{Roug-Ref-NoPrunDijk}}(s, t)$  is the path result returned by algorithm *Roug-Ref-NoPrunDijk*.*

*Proof.* The difference between *Roug-Ref-NoPrunDijk* and *Roug-Ref* is that in the former one, we do not use the node information for pruning out in Dijkstra's algorithm in the error guaranteed path refinement step of algorithm *Ref*. This will only affect the total running time and the total memory usage. Thus, we only prove the total running time and the total memory usage.

Firstly, we prove the *total running time*. (1) In most of the cases, there is no need to use the error guaranteed path refinement step in algorithm *Ref*. In this case, the total running time is the sum of the running time using algorithm *Roug* and the first three steps in algorithm *Ref*. From Theorem 2, Theorem 3 and Theorem 4, we obtain the total running time  $O(n \log n + l)$ . (2) In some special cases, we need to use the error guaranteed path refinement step in algorithm *Ref* for error guarantee. Since we do not use the node information for pruning out in Dijkstra's algorithm in the error guaranteed path refinement step of algorithm *Ref*, we need to perform Dijkstra's algorithm on the weighted graph  $G_{\text{Ref}}$  constructed by the original Steiner points (i.e.,  $k_{SP} = O(\log \frac{LN}{\epsilon})$  Steiner points per edge) and  $V$  in the error guaranteed path refinement step, and the running time is  $O(n \log \frac{LN}{\epsilon} \log(n \log \frac{LN}{\epsilon}))$ , so we obtain the total running time  $O(n \log \frac{LN}{\epsilon} \log(n \log \frac{LN}{\epsilon}) + l)$ . (3) In general, the total running time is  $O(n \log \frac{LN}{\epsilon} \log(n \log \frac{LN}{\epsilon}) + l)$ .

Secondly, we prove the *total memory usage*. (1) In most of the cases, there is no need to use the error guaranteed path refinement step in algorithm *Ref*. In this case, the total memory usage is the sum of the memory usage using algorithm *Roug* and the first three steps in algorithm *Ref*. From Theorem 2, Theorem 3 and Theorem 4, we obtain the average case total memory usage  $O(n + l)$ . (2) In some cases, we need to use the error guaranteed path refinement step in algorithm *Ref* for error guarantee. Since we do not use the node information for pruning out in Dijkstra's algorithm in the error guaranteed path refinement step of algorithm *Ref*, we need to perform Dijkstra's algorithm on the weighted graph  $G_{\text{Ref}}$  constructed by the original Steiner points (i.e.,  $k_{SP} = O(\log \frac{LN}{\epsilon})$  Steiner points per edge) and  $V$  in the error guaranteed path refinement step, and the memory usage is  $O(n \log \frac{LN}{\epsilon})$ , so we obtain the total memory usage  $O(n \log \frac{LN}{\epsilon} + l)$ . (3) In general, the total memory usage is  $O(n \log \frac{LN}{\epsilon} + l)$ .  $\square$